STRUCTURAL STUDY OF PENNSYLVANIA HISTORIC BRIDGES   HAER No. PA-478
Pennsylvania Historic Bridges Recording Project
Pennsylvania Department of Transportation
Harrisburg
Dauphin County
Pennsylvania

PHOTOGRAPHS

WRITTEN HISTORICAL AND DESCRIPTIVE DATA

HISTORIC AMERICAN ENGINEERING RECORD
National Park Service
1849 C Street, NW
Washington, DC 20240

HISTORIC AMERICAN ENGINEERING RECORD

STRUCTURAL STUDY OF PENNSYLVANIA HISTORIC BRIDGES

HAER No. PA-478

Location:	Pennsylvania Department of Transportation, Harrisburg, Dauphin County, Pennsylvania.
Dates of Construction:	1890, 1904, 1906.
Designer:	Various — see HAER documentation for individual structures.
Builder:	Various — see HAER documentation for individual structures.
Present Use:	Vehicular bridges.
Present Owner:	Pennsylvania Department of Transportation.
Significance:	One metal lattice truss bridge (1890) and two reinforced concrete arch bridges (1904 and 1906) were selected for engineering analyses and evaluation based on modern structural theory and structural theory at the time the bridges were built.
Engineers:	Stephen G. Buonopane and Dr. Dario A. Gasparini, August 1997.
Project Information:	This report is part of the Historic American Engineering Record (HAER) Pennsylvania Historic Bridges Recording Project - I, co-sponsored by the Pennsylvania Department of Transportation (PennDOT) and the Pennsylvania Historical and Museum Commission during the summer of 1997. The project was supervised by Eric DeLony, Chief of HAER. Dr. Dario A. Gasparini, Professor of Civil Engineering at Case Western Reserve University (Cleveland, Ohio), and Stephen G. Buonopane completed this project under contract with HAER.

See HAER No. PA-460 for documentation of the Upper Bridge at Slate Run (1890).

See HAER No. PA-471 for documentation of the Frankford Avenue Bridge (1904).

See HAER No. PA-451 for documentation of Campbell's Bridge (1906).

TABLE OF CONTENTS

PART I: Metal Lattice Truss

1. INTRODUCTION

J. G. James and Gregory K. Dreicer provide recent studies on the evolution of wood and iron lattice bridges.[1] Dreicer examines the lattice form as an example of "intercultural exchange in building technology." James and Dreicer concur that, although precursors existed, the lattice form became widely used because of Ithiel Town, who received a U.S. patent for a lattice bridge on 28 January 1820. Town published brochures, placed newspaper advertisements and published in technical journals to promote his lattice designs.[2] Town also traveled extensively, including two journeys to Europe (one in 1829-30), further disseminating his design ideas.

James states that

> the true iron lattice bridge finally appeared in Ireland in the 1840s through John Benjamin MacNeill (c. 1793-1880) who, as chief engineer to several Irish railways, turned to the lattice beam, which he decided on constructing of iron instead of following the American practice of timber.[3]

MacNeill's first iron lattices were made for the Dublin & Drogheda Railway, beginning with an 84'-long road bridge over the line at Rahent near Dublin, built in 1843-44. In 1849 William T. Doyne designed a 156'-long lattice road bridge over the Rugby & Leamington Railway.[4] James notes that "by 1850 iron lattice bridges with spans up to 100' were too common to receive mention in the literature."[5] In 1851, Doyne and Blood published a paper in the *ICE Proceedings,* describing procedures used for the design of lattice bridges (and Warren trusses).[6] The published discussions of that paper reveal some of the issues regarding the principal structural forms used for bridges at the time: the Warren truss, the lattice truss and riveted plate or box girders. Doyne advocated lattice trusses and stated that he had constructed a 140'-long lattice bridge to carry a railway over the River Taff. Comparing lattice trusses with plate girders, Doyne noted that "the sectional area of the top and bottom must be identical in either case" but that

---

[1] J. G. James, "The Evolution of Iron Bridge Trusses to 1850," *Transactions of the Newcomen Society* 52 (1980-81): 67-101; ibid., "The Evolution of Wooden Bridge Trusses to 1850," *Journal of the Institute of Wood Science* 9 (June 1982): 116-35; (December 1982): 168-93; G. K. Dreicer, "The Long Span: Intercultural Exchange in Building Technology," Ph.D. diss., Cornell University, May 1993.

[2] Ibid.

[3] James, "The Evolution of Iron Bridge Trusses to 1850."

[4] Ibid.

[5] Ibid.

[6] W. T. Doyne and W. B. Blood, "An Investigation of the Strains Upon the Diagonals of Lattice Beams, with the Resulting Formulae," *ICE Proceedings* 11 (1851): 31-14.

the method of uniting them by the diagonal struts and ties, which were comparatively small pieces of cheap and easily handled rolled merchant bar iron, simply punched at the ends and at the intersections for the rivets, was a simpler and easier system, than riveting together a number of sheets of iron....

Doyne also advocated lattice trusses over Warren trusses because for longer spans, "smaller-sized bars and rivets were required in contrast with Warren trusses for which

large dimensions of iron must be adopted, the pins would require to be very strong, and the holes must be cut out by expensive machines instead of by a simple punching press. In deep girders, it was convenient to place the platform or roadway, midway of the depth, which just suited the lattice form, but was not so convenient with the simple triangulation.[7]

The lattice form was thus viewed as more practical and economical. James M. Rendel and Isambard Kingdom Brunel, in their discussions, noted that the forces in the diagonals could not be determined exactly using only force equilibrium and thus for the lattice "much of the material employed was useless" whereas for a Warren truss, "every part was made to perform its duty, either bearing pressure, or in tension." The statical indeterminacy of the lattice truss may partially explain the fact that "France took surprisingly little interest in the iron lattice bridge" and Cullmann's generally unfavorable assessment of lattice trusses.[8] Despite Cullmann's judgment, the lattice truss became popular in Germany and Austria. James states that:

A tiny bridge over the Neisse at Guben (1846) is usually cited as the first continental example. A larger one followed over the Wupper at Rittershausen (22.8 m trusses, 1847) which had diagonal stays like the Dublin bridge. Further examples in 1848 include those over the Saale at Grisehna on the Magdeburg-Leipzig line and over the Elbe at Magdeburg.[9]

Dreicer provides a chronological list of lattice bridges built throughout the world, especially in Russia and India.[10]

---

[7] Ibid.

[8] James, "The Evolution of Iron Bridge Trusses to 1850"; K. Cullmann, "Der Bau der Hölzernen Brücken in den Vereinigen Staaten von Nordamerika," *Allgemeine Bauzeitung mit Abbildungen* (Vienna, Austria) 16 (1851): 69-129.

[9] James, "The Evolution of Iron Bridge Trusses to 1850."

[10] Dreicer.

In contrast, in the U.S. by 1850 the lattice form was largely eclipsed by the patented truss forms of S. H. Long, W. Howe and T. and C. Pratt (see Gasparini and Simmons).[11] Dreicer examines some of the reasons for this development in American bridge design practice. A basic difference between Town's lattice design and the trusses of Long, Howe and Pratt, is that the latter trusses were prestressed and allowed for tightening if a bridge loosened from dimensional changes in wood; a lattice truss was neither prestressed nor adjustable. The "non-positive" connections for the wood diagonals give the Howe truss a distinct advantage for wood construction.[12] Although this advantage is not as significant for iron, American engineers adopted the familiar Howe truss for the first U.S. all-iron railway trusses.

It appears that the all-iron lattice form was reintroduced into the U.S. by the engineer Howard Carroll, who became an assistant to George E. Gray, chief engineer for the New York Central Railroad. Snow remarks that the New York Central adopted the riveted lattice

> through the influence, if I am not mistaken, of Howard Carroll (killed in battle during the war), one of (Gray's) assistants, a brilliant young Irish engineer, who had been brought up under Sir John MacNeill, and was therefore thoroughly imbued with English ideas.[13]

In 1859 Howard Carroll built an all-wrought-iron, all-riveted, lattice railway bridge over the Mohawk River at Schenectady. The bridge was a deck lattice of ten 67'-0" spans.[14] Gray also states that the first specifications for riveted bridgework were written by Carroll in 1857.[15] The tradition begun by Carroll and Gray was continued by Gray's successor, Charles Hilton, working with George H. Thomson. Thus the riveted lattice became the standard truss design for the New York Central Railroad from 1859 to about 1890. As noted by Dreicer, little is known about the thirty-year development of lattice trusses by New York Central engineers.[16] Vose describes the methods used for analysis and design and provides an admiring description of the Canestota Station bridge (see Figure 1).[17] The papers of Gray and Thomson provide a glimpse on the

---

[11] Dario Gasparini and David Simmons, "American Truss Bridge Connections in the Nineteenth Century, Parts I and II," *Journal of Performance of Constructed Facilities* 11, No. 3 (1997): 119-29, 130-40.

[12] Dreicer.

[13] J. P. Snow, "Report of AREA Committee XV on Iron and Steel Structures," *Proceedings, Sixth Annual Convention of the AREA* (Chicago: American Railway Engineering Association, 1905), 197-217.

[14] G. E. Gray, "Notes on Early Practice in Bridge Building," *Transactions of the American Society of Civil Engineers* 37 (1897): 1-16; Snow.

[15] Gray.

[16] Dreicer.

[17] G. L. Vose, *Manual for Railroad Engineers and Engineering Students* (Boston: Lee and Shepard, 1878).

number of lattice bridges built by the New York Central Railroad.[18] All this bridge-building activity was largely ignored in Cooper's 1889 history because Cooper was a proponent of mainstream, "American pin-jointed trusses."[19] Dreicer notes that

> New York railroads in 1891 had hundreds of riveted iron lattice bridge spans. Of the largest railroads in the state; the New York Central and Hudson Railroad, out of a total of 177 bridges, most built during the thirty previous years, 33 were lattice; on the Delaware and Hudson Railroad, out of 88 bridges, 32 were lattice bridges.[20]

This New York practice of building lattice bridges apparently waned in the 1890s. Dreicer cites the following 1891 quote from William E. Rogers, Chairman of the Board of Railroad Commissioners of the State of New York:

> In the early days of bridge building, particularly of iron bridges, it was the habit to construct trusses of complicated forms, the accurate calculation of the strains on which it is very difficult, in some cases impossible, to compute. An approximation close enough for practical purposes is always reached, however. A better practice now prevails, and trusses of simple form, admitting of no ambiguity, are alone accepted by the best engineers. In exceptional cases complex trusses have to be resorted to but they are avoided as much as possible.[21]

Rogers' reference to a "better practice" clearly means the mainstream "American pinned trusses." Lattice trusses had lost their champion.

The lattice truss used for the Upper Bridge at Slate Run (see Figure 2) in Brown Township, Lycoming County, Pennsylvania, is clearly related to the New York Central Railroad tradition. A brief evaluation of its structural design and structural behavior follows.

## 2.	MATERIAL PROPERTIES

A short length of a bar, with a cross-section of 1-1/2" by 3/8", was found at the site of the Upper Bridge at Slate Run. The piece may have been part of an original railing. A tensile specimen was machined from the bar and tested at the Civil Engineering Department of Case Western Reserve University. Figure 3 shows the uniaxial stress-strain curve for the material. It shows a yield stress of 40 kilopounds per square inch (ksi), a tensile strength of 51 ksi and an

---

[18] Gray; G. H. Thomson, "American Bridge Failures," *Engineering* 46 (14 September 1888): 252-83.

[19] T. Cooper, "American Railroad Bridges," *Transactions of the American Society of Civil Enginners* 21 (1889): 1-54.

[20] Dreicer.

[21] C. F. Stowell, ed., "Strains on Railroad Bridges of the State," *Report of the Board of Commissioners of the State of New York* (Albany: Weed, Parsons & Co., 1891); cited in Dreicer, "The Long Span."

ultimate strain of 0.18.[22] The entire stress-strain curve matches, almost precisely, that given by M. O. Withey and J. Aston for 3/8"-diameter wrought-iron rods tested in 1888. In addition, the fracture surface was distinctly fibrous, which is characteristic of wrought iron.[23] The fracture surface was examined using an analytical scanning electron microscope at the Department of Materials Science and Engineering at Case Western Reserve University. Figure 4 is a magnified image of the fracture surface. The fibrous phase is almost pure iron. The phase labeled "A," which has sharp (brittle) fracture surfaces, is slag. Analysis of the overall surface indicates a 97.7 percent iron content. Analysis of phase A indicates a high content of silicon (9.7 percent), phosphorus (6.1 percent) and manganese (2.9 percent), which is typical of slag. Such a microstructure is a consequence of the method used to make wrought iron.

The production and processing of wrought iron are described by Withey and Aston. Up to about 1930 most wrought iron was produced by a "puddling" and rolling process, as follows. A hearth-type furnace was charged with pig iron, which was heated using coal as a fuel. As the pig iron melted, the hot gases from the burning fuel oxidized carbon from the iron, which had an initial carbon content of 3.5 to 4 percent. As melting continued to completion, roll scale (magnetic iron oxide) was added to oxidize most of the carbon, silicon, sulfur, phosphorus, and manganese from the fluid iron; the oxides then became part of the slag. During the oxidation of the impurities, the molten iron was agitated manually by an operator using a long steel rod. As purification continued, the melting point of the iron climbed (from about 1200 to 1500 degrees Celsius) until the operator, or puddler, was no longer able to agitate the pasty iron interspersed with fluid slag. At that point the sponge-like ball of iron-slag mixture was removed from the furnace dripping with slag, which was fluid at the finishing temperature. Ninety-seven to ninety-eight percent of the fluid slag was removed by rolling the puddle ball into flat "muck tears" about 3/4" by 3" to 6" in cross section. Practically all the silicon, phosphorus and manganese in wrought iron are associated with the 2 to 3 percent of occluded slag which was not removed in the rolling. The slag contains 60 to 80 percent of the oxides or iron, 15 to 30 percent of silica, together with the oxides of manganese and phosphorus.[24] Further density and homogeneity was imparted to the iron by hot working of the muck bars. In making bars and billets the muck bars were cut into short lengths, stacked in rectangular piles with long axes parallel and bound with iron wires. The pile was then heated to a welding temperature and rolled into bars. A second cutting, piling, reheating, and rolling was often performed before the bars were worked into final shape. For plates and sheets the muck bars were stacked in large rectangular piles with alternate layers running cross-wise of the pile in order to increase the strength of the metal in planes

---

[22] M. O. Withey and J. Aston, *Johnson's Materials of Construction*, 5th ed. (New York: John Wiley and Sons, 1919).

[23] Ibid.

[24] Ibid.

perpendicular to the rolling.[25] Such processing produced wrought iron with hundreds of thousands of "slag fibers" per square inch. The chemically inert and discontinuous slag fibers imparted excellent corrosion resistance to wrought iron.[26]

In summary, because of the observed microstructure and the uniaxial stress-strain properties, the material found at the site of the Upper Bridge at Slate Run is definitely wrought iron.

3. CONCEPTUAL DESIGN AND DETAILING

3.1. Geometry

The height-to-span ratio of the Upper Bridge at Slate Run is approximately 8, which is not an atypical value for turn-of-the-century bridges. The endmost panels of the truss are different lengths (9.0' and 13.6'), introducing a slight asymmetry to the bridge. In addition, the diagonal members intersect at an angle slightly different than 90 degrees. Finally, the truss is composed of five diagonal systems of bracing (see Figure 6), rather than the more typical four systems in a metal lattice bridge. The use of five diagonal systems also has the effect of placing the panel points along the upper chord halfway between the locations of the panel points in the lower chord. No sound explanations have been found for these unusual geometric features. Location and study of original design documentation from this bridge, or one with similar features, might provide some insight on the unusual geometry.

3.2. Floor Beam to Lower Chord Connection

Figure 5 shows schematically a typical connection between a transverse floor beam and the lower chord.[27] The floor beam is attached to the inner vertical plate of the bottom chord, and thus transfers its load to the chord with some eccentricity. A small diagonal strut is added from the inner chord plate to the center of the bottom plate. This strut is undoubtedly an attempt to try to apply the vertical force from the floor beam to the center line of the lower chord, thereby preventing any torsional moment due to the eccentric application of the vertical force. Assessment of the effectiveness of the strut would require a detailed, three-dimensional finite element study which is beyond the scope of this report.

However, it is possible to estimate some of the force effects of the eccentric floor beam loading, neglecting the effect of the diagonal strut. Figure 3 also shows an exploded view of the cross-section with forces due to the roadway load of 80 pounds per square foot (psf). The

---

[25] Ibid.

[26] Ibid.

[27] U.S. Department of the Interior, Historic American Engineering Record (HAER), No. PA-460, "Upper Bridge at Slate Run," 1997, drawing sheet 4, Prints and Photographs Division, Library of Congress, Washington, D.C.

cccentric load from the floor beams will produce axial tension in the floor beams and axial compression in the top lateral bracing system. Due to the height of the truss, the magnitude of these axial forces are relatively small, only about 200 pounds. This analysis assumes that the lattice formed by the interconnecting truss diagonals is strong enough to prevent any differential rotation between the upper and lower chords.

3.3. Static Determinacy

Given a particular loading condition, the forces within a statically determinate structure may be determined from equations of equilibrium alone. In a statically indeterminate structure, geometric compatibility equations between joint displacements and material stress-strain equations must be satisfied in addition to those of equilibrium. For a planar truss, exactly two equations of equilibrium exist for each joint. Therefore, if the number of force unknowns equals twice the number of joints, all unknown forces may be determined from equilibrium alone. If the number of unknown forces exceeds the number of equilibrium equations, the truss is indeterminate. Each degree of indeterminacy adds an additional compatibility equation to the group of equations which must be solved simultaneously. Thus the degree of indeterminacy may be considered as a measure of the computational effort necessary to determine all of the member forces within a structure. Today the use of computers has made commonplace the solution of structures many hundreds of times indeterminate. Structural engineers of the nineteenth and early twentieth centuries could only analyze highly indeterminate structures using approximate methods, due to practical limitations of manual calculation.

The degree of indeterminacy, n, of a planar truss is given by the simple formula

$$n = m + r - 2j \tag{1}$$

where:

m = number of members,
r = number of support reactions,
j = number of joints.[28]

An elevation of one of the trusses from the Upper Bridge at Slate Run appears in Figure 2. Crossing diagonals may be assumed to act independently at their points of intersection between the upper and lower chords.[29] The thirty-seven chord members and forty-two diagonals give $m = 79$. There are three support reactions: a vertical force at panel point L0 and vertical and horizontal forces at panel point L19. Finally, thirty-nine joints results in a static indeterminacy of degree four. It is not practical to do an exact, *manual* analysis of a truss that is statically indeterminate to the fourth degree.

---

[28] A. Ghali and A. M. Neville, *Structural Analysis* (London: Chapman and Hall, 1989), 9.

[29] See "Intersections of Diagonals" section.

3.4.   Approximate Structural Analyses

Lattice trusses were most often designed by treating the lattice as a series of independent Warren trusses which could be analyzed separately as statically determinate sub-structures. The results of each analysis were combined to provide the forces necessary to design the members of the full lattice truss.[30] Figure 6 shows the five Warren trusses which compose the lattice of the Upper Bridge at Slate Run. More often a lattice truss is composed of four Warren trusses, and therefore referred to as a Warren "quadrangular" truss. Here the use of five trusses suggests the more accurate term "quintangular."

Each of the five trusses in Figure 6 is statically determinate, and thus member forces and stresses can be calculated from principles of equilibrium alone.[31] Simple addition of the chord forces from each of the five trusses allows for design of the actual chord members. Note that each chord member appears in all five of the trusses, and therefore receives some amount of force from each of the five statically determinate analyses.

The results of such a "five-truss" analysis, as would have been performed by engineers of the late nineteenth century, are compared to a modern computer analysis in order to assess the accuracy of the approximate method. The planar (two-dimensional) computer model consists of beam-column elements capable of carrying axial, shear and moment forces. Beam-column elements are used rather than truss elements (which carry only axial force) in order to include the effects of the rigidity of the riveted connections, even though the influence of such connections is typically small. The solution of the model is obtained using the direct stiffness method. Details of the model geometry and properties appear in Appendix A.

Two load cases are considered:

1.   Dead load and roadway (RW) live load of 80 psf.

2.   Dead load and railroad (RR) load of 1,500 pounds per foot (lb/ft).[32]

Table 1 outlines the dead loads for one lattice truss. Table 2 lists several members used for comparison and representative of the overall behavior of the lattice truss. Table 3 compares results of the approximate "five-truss" analysis with the modern computer analysis. In all cases the approximate analysis produces acceptable results, never differing more than 10 percent from the computer analysis, and more often substantially less than 10 percent.

---

[30] G. L. Vose, *Manual for Railroad Engineers* (Boston: Lee and Shepard, 1878), 252-62; J. B. Johnson, C. W. Bryan, and F. E. Turneaure, *The Theory and Practice of Modern Framed Structures*, 9th ed., vol. 1 (New York: John Wiley and Sons, 1914), 176; M. Merriman and H. S. Jacoby, *Roofs and Bridges*, 6th ed., pt. 1 (New York: John Wiley and Sons, 1922), 197-203.

[31] See "Static Determinacy" section.

[32] For roadway loads see M. Merriman and H. S. Jacoby, *Roofs and Bridges*, 5th ed., pt. 3 (New York: John Wiley and Sons, 1920), 92-94; for railroad loads see Vose.

Table 1 Dead load for one truss, Upper Bridge at Slate Run.

Item	Weight (kips)
Structural Steel	83.8
Top Bracing	2.8
Bottom Bracing	1.1
Floor Beams	12.5
Subtotal	100.2
Add 5 percent for rivets and connections	105.2
Stringers and flooring (estimate 100 lb/ft)	20.0
Total dead load	125.2
1/3 dead load to upper chord	41.7
Over 19 panel points	2.20
2/3 dead load to lower chord	83.5
Over 20 panel points	4.18

Table 2 Members of interest, Upper Bridge at Slate Run.

Member	Location
Upper chord mid-span	U9-U10
Lower chord mid-span	L9-L10
End post	L0-U1
Compression diagonal near support	L1-U4
Tension diagonal near support	L15-U18
Diagonal near mid-span	L9-U7

Note: See Figure 2 for locations.

The lattice truss may also be considered as a beam where the chords form the flanges and the lattice diagonals form the web. Dividing the total dead load of 125.2 kilopounds (kips) by the span gives a uniform load $w = 0.62$ lb/ft. The roadway live load of 80 psf applied across half the width of the bridge gives a uniform live load $w = 0.72$ lb/ft. The maximum moment, M, at the center of the span may be found from $M = wl^2/8$, giving a moment of 6,874 kip-ft. Dividing the moment by the height of 25'-0" between the upper and lower chords gives an estimate of the axial forces in the chords of 275 kips. This value compares well with the axial forces in members U9-U10 and L9-L10 found by computer analysis (see Table 3).

Table 3 Comparison of approximate and computer analyses of Upper Bridge at Slate Run.

Load Condition: DL + LL(RW)			
Member	Force (kips)		
	5-Truss*	Computer*	Difference**
U9-U10	-274.1	-273.3	0.9
L9-L10	261.0	261.3	-0.3
L0-U1	-86.3	-83.1	3.2
L1-U4	-25.1	-22.0	3.1
L15-U18	31.4	33.9	-2.5
L9-U7	9.5	10.0	-0.4

Load Condition: DL + LL(RR)			
Member	Force (kips)		
	5-Truss*	Computer*	Difference**
U9-U10	-438.5	-437.2	1.4
L9-L10	414.0	414.5	-0.5
L0-U1	-138.2	-133.0	5.2
L1-U4	-39.1	-34.1	5.0
L15-U18	50.9	55.0	-4.1
L9-U7	16.1	16.8	-0.7

Notes:

*   Negative force indicates compression.

**   Negative difference indicates five-truss analysis is unconservative.

4.   STRUCTURAL BEHAVIOR

4.1.   Intersections of Diagonals

Figure 7 shows two ideal truss members (carrying only axial forces) joined at a node and intersecting at a given angle, α. A local x-y coordinate system is defined as shown, the x-axis aligned with one of the diagonals. Equilibrium in the x and y directions, respectively, gives

$$F_1 + F_2 + (F_3 + F_4)\cos\alpha = 0 \tag{2}$$

$$(F_3 + F_4)\sin\alpha = 0 \tag{3}$$

From Equation (3), since $\sin\alpha \neq 0$ for an arbitrary α, the quantity $F_3 + F_4$ must equal zero. Substituting $F_3 + F_4 = 0$ into Equation (2) gives $F_1 + F_2 = 0$. Therefore the axial forces in the

diagonals remain unchanged on either side of the joint, provided no external load is applied at that joint. Since there can be no force interaction between the diagonals, the truss may still be accurately analyzed by assuming that diagonals are not connected at their points of intersection.

To verify the assumption of independent behavior of the diagonals, two computer models of the truss are analyzed for the case of a unit load at joint L9 on the lower chord. The first model places a joint at every intersection point, interconnecting the diagonals; while the second uses independent diagonals. In both cases all members are modeled as beam-column elements capable of carrying axial, shear and moment forces. Details of the computer model appear in Appendix A. The results of the two analyses, summarized in Table 4, show the effects of interconnection to be negligible. This close correspondence reveals that even though the diagonals are connected with riveted plates at their intersections, their behavior remains nearly independent.[33] The slight differences in the results may be attributed to the ability of the members in the computer model to carry shear and bending forces, whereas Equations (2) and (3) strictly apply to ideal truss members only.

Table 4 Effect of diagonal interconnections, Upper Bridge at Slate Run.

Load Condition: Unit Load at L9		
Panel point	Displacement (inches) with:	
	Diagonals Interconnected	Diagonals Independent
L9	0.0108	0.0109
Member	Force (kips) with:	
	Diagonals interconnected	Diagonals independent
U9-U10	-2.039	-2.042
L9-L10	1.540	1.534
L0-U1	-0.251	-0.244
L1-U4	-0.039	-0.031
L15-U18	0.212	0.212
L9-U7	0.472	0.469

4.2. Coupling of Diagonal Systems

The previous section demonstrates that the five individual trusses do not interact through the diagonal interconnections. Therefore any interaction must occur through the chords, which

---

[33] U.S. Department of the Interior, Historic American Engineering Record (HAER), No. PA-460, "Upper Bridge at Slate Run," drawing sheet 5.

are common among all five sub-trusses (see Figure 6). Figure 8 shows conceptually the transfer of force from one diagonal system to another. The load at a lower chord panel point applied is carried by a diagonal in tension to the upper chord. Some component of that force is transferred to the upper chord, and since the chords are common to all five trusses, some force can be transferred to another diagonal system. However, the majority of the load remains within the chord up to the supports.

In order to quantify the amount of interaction between trusses, a series of analyses is performed in which a unit load is placed at each of the lower panel points (L1-L18). Using the model of the full lattice truss, the vertical components of the member forces in the end-most diagonals of each of the five trusses are calculated.[34] The sums of these vertical components from each end of the truss are given in Table 5. Figure 9 shows two axial force distributions in the diagonals for unit loads at panel points L4 and L8. When the load is applied near the ends of the truss, more of the applied load tends to remain within the truss system to which the loaded panel point belongs. A unit load applied near the center of the truss will tend to distribute more of its load to neighboring truss systems.

For example, a unit load of 1 kip is placed at L4. According to Figure 6, this node is a part of Truss 4. The end-most diagonals of Truss 4 are L0-U2 and U17-L19, in which the vertical components of the axial force are found to be 0.43 kips and 0.07 kips. Thus, of the unit load placed at L4, a total of 0.50 kips appears in the truss at its end-most members; the remaining 0.50 kips is distributed amongst the other four trusses. If no interaction occurred the entire applied load of 1.00 kips would appear in the end diagonals of the loaded truss. Figure 10 shows the results from the series of analyses, and reveals that more interaction occurs for loads placed near the center of the truss than for loads placed near the ends.

---

[34] The endmost diagonal is defined as the last member unique to that truss system. See Figure 2.
The endmost diagonals are:
Truss 1   U1-L1   L16-U19
Truss 2   U1-L2   L17-U19
Truss 3   U1-L3   L18-U19
Truss 4   L0-U2   U17-L19
Truss 5   L0-U3   U17-L19

Table 5 Unit load analysis of truss coupling, Upper Bridge at Slate Run.

Panel point with unit load	Number of truss with loaded panel point	Sum of vertical force components in end diagonals of loaded truss (kips)
L1	1	0.79
L2	2	0.72
L3	3	0.57
L4	4	0.50
L5	5	0.44
L6	1	0.37
L7	2	0.38
L8	3	0.33
L9	4	0.35
L10	5	0.35
L11	1	0.34
L12	2	0.38
L13	3	0.34
L14	4	0.46
L15	5	0.52
L16	1	0.58
L17	2	0.72
L18	3	0.73

4.3.   Bracing of Compressive Diagonals

The reduction of compression capacity in a member due to buckling is controlled by its slenderness, or the ratio of length to radius of gyration, l/r.[35] Out-of-plane buckling occurs when the compression member deforms such that it bows out of the plane of the truss. In-plane buckling occurs when the member bows within the plane of the truss. A compression member's overall load capacity is determined by the direction with the greater slenderness ratio. An efficiently designed compression member will have in-plane and out-of-plane slenderness ratios that are almost equal.

---

[35] Radius of gyration is the square root of the ratio of a section's moment of inertia to its cross-sectional area. See S. Timoshenko and G. H. MacCullough, *Elements of Strength of Materials,* 3rd ed. (New York: Van Nostrand, 1949), appendix B.

Table 6 lists the slenderness properties for the laced compression diagonals. (See Appendix A for the location of member types within the truss.) All of the compression members are formed from angle sections laced together. The lacing causes the angles to act together in the out-of-plane direction thereby giving a large radius of gyration which offsets the long out-of-plane unbraced length. For the in-plane direction, the compression diagonals have relatively small radii of gyration and therefore need to be braced along their length. At their interconnections, the tensile diagonals brace the compressive diagonals against in-plane buckling. For section type CD-1 (see Table A-3 in Appendix A) the slendemesses in each direction are nearly identical (67 and 69), and even for the other sections types the slenderness values are of commensurate magnitude, evidence of well-designed compression elements. For the slenderness ratios in Table 6, modern design codes would allow an average compressive design stress of about 70 percent of the yield stress (not including any factors of safety).

Table 6 Slenderness of Compression Diagonals, Upper Bridge at Slate Run.

Section type*	Radius of gyration, r (inches)		Slenderness ratio = unbraced length**/r	
	Out-of-plane	In-plane	Out-of-plane	In-plane
CD-1	6.55	1.27	67	69
CD-2	6.32	1.02	69	86
CD-3	6.40	1.03	68	85
CD-4	6.41	0.90	68	97
CD-5	6.48	0.91	67	96

Notes:

* See Appendix A for section types.

** Unbraced lengths: 36.43' out-of-plane, 7.29' in-plane.

4.4. Axial Stresses

Computer analyses of the truss are performed under realistic loading conditions to determine member stresses. Dead and live load magnitudes and combinations are detailed in the previous section. Figure 11 shows axial force distributions for the truss chords and diagonals for dead load and roadway live load. Note that maximum chord forces occur at the center of the span, while maximum diagonal forces occur at the ends of the span. The results for a representative group of members appear in Table 7. Typical allowable stresses from contemporary (1880s) engineering literature are 10 ksi for tension members, 6 ksi for compression diagonals and 8 ksi for compression chord members.[36] Note that compression

---

[36] Vose.

members are assigned a lower allowable stress than tension members due to the possibility of buckling, as previously discussed. In addition, the diagonal compression members have lower allowable stresses than the chord members, because diagonals typically would be more slender than chords. The principle of reducing the allowable stress for members in compression is still in use in modern steel design.

For the roadway loading condition the axial stresses are generally well below the allowable limits. Even for the railroad loading the members are below, or only slightly above (e.g., member U9-U10), the typical allowable stresses cited. The general magnitudes of member stresses under railroad loading suggests that the bridge was originally designed for loads significantly greater than roadway loads. No direct evidence has been found that the bridge was once a railroad bridge, but the bridge has been closely tied to railroad interests and a logging industry active in the area at the turn of the century.[37]

Table 7 Axial forces and stresses, Upper Bridge at Slate Run.

Member	Force (kips)		Area (in^2)	Stress (ksi)	
	DL+LL(RW)	DL+LL(RR)		DL+LL(RW)	DL+LL(RR)
U9-U10	-273.25	-437.15	51.75	-5.28	-8.45
L9-L10	261.30	-414.46	46.25	5.65	8.96
L0-U1	-83.12	133.03	29.75	-2.79	-4.47
L1-U4	-21.97	-34.05	5.63	3.90	-6.04
L15-U18	33.86	54.95	5.63	6.01	9.75
L9-U7	9.95	16.80	4.22	2.36	3.98

Note: Negative force or stress indicates compression.

5.   OBSERVATIONS

Comparison between the lattice truss of the Upper Bridge at Slate Run and the Canestota Bridge shows common features that suggest the involvement of the New York Central Railroad in the design and construction of the Upper Bridge at Slate Run. A study of these two bridges, as well as other lattice trusses known to have been used by the New York Central, which focuses on features such as geometry and details of connections and riveting, might clarify the role of the New York Central Railroad as well as explain certain geometric features of the Upper Bridge at Slate Run.

One such unique detail is the diagonal strut at the floor beam to lower chord connection. The strut is clearly intended to reduce eccentricity of the load application to the lower chord. More detailed engineering studies of this connection are required to assess the effectiveness of

---

[37] See Withey and Aston for allowable stresses; HAER No. PA-460 for railroad and logging interests.

this strut. Nevertheless, the success of this lattice truss bridge suggests that the floor beam to chord connection is a sound detail, regardless of the effectiveness of the strut.

The plaques over the bridge's portals state that it was built by the Berlin Iron Bridge Company. However, the extent of involvement of the Berlin Iron Bridge Company in the design, fabrication and construction of this lattice bridge is unclear. Further historical research will provide a greater understanding of the role of the Berlin Iron Bridge Company (well-known at the time for their use of lenticular trusses) and their relationship to the New York Central (designers and constructors of many other lattice truss bridges).

The approximate methods used by engineers of the late nineteenth century to design lattice truss bridges provide extremely accurate results when compared to a modern structural analysis. Further, the modern analyses presented here show the axial stress levels to be of reasonably uniform magnitude throughout the various parts of the bridge. Such consistency attests to proper variation of member sizes and properties within the truss as well as to the soundness of the overall design.

PART II: Reinforced Concrete Arch Bridges

1.   INTRODUCTION

A HAER study of historic Iowa bridges provides an introduction to the development of reinforced concrete arch bridges in the United States.[38] The pioneering 1894 reinforced concrete arch at Rock Rapids, Iowa, is the source of an important lineage of reinforced concrete design in the United States, defined by the work of the Concrete-Steel Engineering Co. In the first decade of the twentieth century there was an explosive growth in the use of concrete. Edwin Thacher, writing in 1905, boasted:

> Since that date (1894), the Concrete-Steel Engineering Company of New York City and their predecessors have built, or are now building, under the Melan, Thacher and von Emperger patents, about three hundred spans of concrete-steel bridges, distributed over nearly all parts of the United States.[39]

It is within this context of "concrete madness" that two reinforced concrete bridges built in Bucks County in 1904 and 1906 are studied. The 1904 bridge is a closed-spandrel arch, the traditional form for masonry. It has centered, latticed reinforcement whose effectiveness does not depend on the bonding between concrete and steel.[40] The 1906 bridge is an open-spandrel arch, a form that became dominant for concrete in the 1920s and 1930s. It is reinforced with (unlatticed) deformed bars whose effectiveness depends on the bond between concrete and steel. Thus the two bridges represent an evolution in concrete arch forms and in understanding of the behavior of reinforced concrete.

2.   FRANKFORD AVENUE BRIDGE

2.1.   Conceptual Design

Figure 12 shows the reinforced concrete bridge built over Poquessing Creek in Bucks County, completed in November 1904. It is a closed-spandrel, fixed-fixed arch with a span of 71'-0" (21.6 m). The intrados and extrados are circular segments. The reinforcement, latticed and centered within the arch, is essentially the same as that patented by Friedrich von Emperger in 1897 and widely used in the arch bridges of the Concrete-Steel Engineering Co.[41] The

---

[38] U.S. Department of the Interior, Historic American Engineering Record (HAER), No. IA-89, "Structural Study of Reinforced Concrete Arch Bridges," 1997, Prints and Photographs Division, Library of Congress, Washington, D.C.

[39] Edwin Thacher, "Concrete and Concrete-Steel in the United States," *Transactions of the American Society of Civil Engineers* 54, pt. E (1905).

[40] HAER No. IA-89, "Structural Study of Reinforced Concrete Arch Bridges."

[41] Friedrich von Emperger, "Vault for Ceilings, Bridges, etc.," U.S. Patent No. 583,464 (1897).

latticed, centered reinforcement implies that there is no reliance on bonding between steel and concrete to assure effectiveness of the steel.[42]

It is not known whether the Concrete-Steel Engineering Co. had a role in the design of the bridge. Specifications issued in 1903 by the City of Philadelphia and Bucks County do refer to the bridge as a "concrete-steel arch." A special clause requires that "the contractor must pay any royalties that may be legally due for the use of patented methods in the construction of concrete steel arches."[43]

The specifications for the bridge also require that

> The concrete in the arch ring, the coping and the parapets shall be composed of 1 part cement, 2 parts sand or gravel and 5 parts crushed stone. The crushed stone shall be thoroughly mixed from 1/4 inch to 2 inch throughout except in the parapets, where it shall be from 1/4 inch to 3/4 inch in size.

The structural behavior of the arch under various loading conditions is revealed by modeling the bridge and performing structural analyses.

2.2. Structural Behavior

2.2.1. Geometry and Discretization

The arch of the Frankford Avenue Bridge is defined by an intrados of radius 71'-0-11/16" (21.66 m) and an extrados of radius 90'-10-11/16" (27.71 m) (Figure 12). The center of the intrados is located 61'-6-11/16" (18.77 m) below the springline of the arch; the center of the extrados, 18'-6" (5.64 m) below that of the intrados. The axis of the arch may be considered to be the circular arc at mid-depth of the arch of diameter 80'-11-11/16" (24.69 m) with its center half way between the centers of the intrados and extrados. The depth of the arch varies from 16" (0.406 m) at the crown to approximately 38" (0.965 m) at the abutments, measured perpendicular to the arch axis. For computer modeling, the axis of the arch is divided into forty straight segments each 22.05" (0.560 m) long (see Figure 13). Details of the computer model, including nodal coordinates, are given in Appendix B.

The reinforcing steel within the arch consists of ribs formed from two angles 2-1/2" x 2-1/2" x 5/16" at each face, and laced together with steel plates (see Figure 12). The steel rib assemblies are spaced on 3'-10-1/4" centers across the width of the bridge. All analyses are performed on a typical 3'-10-1/4" interior width. Provided there is no significant flexural cracking in the concrete, the steel and concrete will act in parallel due to the lacing and the

---

[42] HAER No. IA-89, "Structural Study of Reinforced Concrete Arch Bridges."

[43] City of Philadelphia and Bucks County, "Specifications for the Construction of a Concrete Steel Arch Bridge on the Line of Frankford Avenue, over Poquessing Creek," 1903.

symmetrical arrangement of the steel within the concrete cross-section.[44] Therefore, the arch is modeled with two parallel elements connecting each node; one with properties of the concrete and one with properties of the steel. The concrete elastic modulus is assumed to be 2,000 ksi and the steel to be 30,000 ksi, giving a modular ratio, n, of 15.[45]

Geometric properties of the sections are listed in Appendix B. Tables 8 and 9 give axial and bending stiffness of the arch sections. It is expected that axial forces, N, will be shared between the steel and concrete approximately in proportion to their axial stiffness, EA, and that bending moments, M, will be shared in proportion to the flexural stiffnesses, EI. Mathematically, the axial force distribution may be expressed as

$$\frac{N_C}{N_S} = \frac{(EA)_C}{(EA)_S} \tag{4}$$

and similarly the moment distribution as

$$\frac{M_C}{M_S} = \frac{(EI)_C}{(EI)_S} \tag{5}$$

In these equations the subscript C refers to concrete elements and S to steel elements.

---

[44] HAER No. IA-89, "Structural Study of Reinforced Concrete Arch Bridges."

[45] F. E. Turneaure and E. R. Maurer, *Principles of Reinforced Concrete Construction*, 4th ed. (New York: John Wiley and Sons, 1932), ch. 10; C. F.. Marsh, *A Concise Treatise on Reinforced Concrete* (New York: Van Nostrand, 1910), 81-82.

STRUCTURAL STUDY OF PENNSYLVANIA HISTORIC BRIDGES
HAER No. PA-478
(Page 23)

Table 8 Axial properties, Frankford Avenue Bridge.

Section No.	Concrete $(EA)_C$ x 10^3 kips	Steel $(EA)_S$ x 10^3 kips	Relative $(EA)_C/(EA)_S$
Crown 1	1,470	175.2	8.39
2	1,480	175.2	8.45
3	1,502	175.2	8.57
4	1,534	175.2	8.76
5	1,576	175.2	9.00
6	1,630	175.2	9.30
7	1,694	175.2	9.67
8	1,770	175.2	10.10
9	1,854	175.2	10.58
10	1,950	175.2	11.13
11	2,056	175.2	11.74
12	2,174	175.2	12.41
13	2,300	175.2	13.13
14	2,438	175.2	13.92
15	2,586	175.2	14.76
16	2,742	175.2	15.65
17	2,910	175.2	16.61
18	3,088	175.2	17.63
19	3,276	175.2	18.70
Spring 20	3,472	175.2	19.82

Table 9 Bending properties, Frankford Avenue Bridge.

Section No.	Concrete $(EI)_c$ x 10^6 k-in^2	Steel $(EI)_S$ x 10^6 k-in^2	Relative $(EI)_c/(EI)_S$
Crown 1	31.44	3.30	9.53
2	32.13	3.39	9.48
3	33.53	3.57	9.39
4	35.71	3.84	9.30
5	38.76	4.23	9.16
6	42.80	4.71	9.09
7	48.01	5.37	8.94
8	54.60	6.18	8.83
9	62.82	7.17	8.76
10	73.00	8.37	8.72
11	85.51	9.81	8.72
12	100.82	11.52	8.75
13	119.46	13.53	8.83
14	142.04	15.90	8.93
15	169.31	18.69	9.06
16	202.08	21.87	9.24
17	241.32	25.56	9.44
18	288.10	29.79	9.67
19	343.66	34.59	9.94
Spring 20	409.40	40.02	10.23

2.2.2. Dead and Live Loads

Dead loads are calculated assuming a concrete density of 150 pounds per cubic foot (pcf) and the steel reinforcing cage estimated to weigh 25 lb/ft. The spandrel areas of the arch were assumed to be filled with earth of density 120 pcf to a level approximately 16 inches above the crown of the extrados. Equivalent nodal dead loads for the arch and fill are given in Appendix B.

Roadway live loads for arches were typically in the range of 80 to 120 psf, representing a 15- to 18-ton truck.[46] Based on the concentrated load possible beneath the rear axle of an 18-ton truck, and including a 25 percent increase for impact, Turneaure and Maurer suggest using a 200 psf uniform live load for design. This live load is positioned over various parts of the bridge to

---

[46] Turneaure and Maurer, 370.

produce maximum positive and negative bending moments at the crown, springing, and quarter points.

2.2.3. Stress Analysis

The results of the five load cases considered are summarized in Tables 10 through 14. All load cases include the dead load applied across the full span. The values given are forces and stresses in the concrete.[47] Figure 14 shows typical axial and bending moment diagrams for load case 5. The maximum overall stresses occur at the springing for load case 5 — a compressive stress of 402 psi at the intrados and a tensile stress of 198 psi at the extrados. A compressive stress of approximately 400 psi should be well below the strength of the concrete used in the bridge. Engineering literature from the early twentieth century suggests common 28-day compressive strengths (f'_c) in the range of 2,000 to 3,000 psi.[48] Typical working compressive stresses in members with combined axial force and bending are $0.40f'_c$.

The tensile stress of 198 psi is likely to be close to the cracking tensile stress of the concrete. However, the live load of 200 psf is a conservative overestimate used for design. An actual service load would more likely be 100 to 150 psf. Also, the next highest tensile stress is only 98 psi, under load case 1 at the extrados of the springing. Therefore the stress analyses of the arch under the various load conditions studied suggest that flexural cracking of the concrete should be minimal.

The largest stress in the steel angles occurs at the intrados of the springing for load case 4 and is equal to 5,100 psi (compression). During the early twentieth century, allowable stresses in steel reinforcement were generally about 50 percent of a yield stress of 32,000 to 34,000 psi.[49] Therefore it may be concluded that the steel remains very lowly stressed under all live loading conditions.

The low stresses in the steel reinforcement are typical of early applications of reinforced concrete. The steel reinforcement was intended to carry both compressive and tensile stresses. The concrete also carried compressive stresses, prevented buckling of the steel and protected it from corrosion. Later development of reinforced concrete as a structural material places the steel reinforcement only in areas where tensile stresses were likely to occur, a more efficient use of material.

---

[47] Sign conventions:
Axial forces and stresses:
$+P$ = tension
$-P$ = compression
Bending moments:
$+M$ = Compression at extrados, tension at intrados
$-M$ = Tension at extrados, compression at intrados

[48] Turneaure and Maurer, ch. 2; Marsh, ch. 2.

[49] Ibid.

Table 10   Load case 1: maximum axial force, Frankford Avenue Bridge.

Location: Springing	
Axial force (kips)	-216
Bending moment (k-ft)	-201
Axial stress (psi)	-124
Bending stress (psi)	-222
Combined stress at intrados (psi)	-346
Combined stress at extrados (psi)	98

Table 11   Load case 2: maximum positive moment at crown, Frankford Avenue Bridge.

Location: Crown	
Axial force (kips)	-150
Bending moment (k-ft)	12
Axial stress (psi)	-204
Bending stress (psi)	76
Combined stress at intrados (psi)	-129
Combined stress at extrados (psi)	-280

Table 12   Load case 3: maximum negative moment at crown, Frankford Avenue Bridge.

Location: Crown	
Axial force (kips)	-148
Bending moment (k-ft)	-10
Axial stress (psi)	-201
Bending stress (psi)	-62
Combined stress at intrados (psi)	-263
Combined stress at extrados (psi)	-139

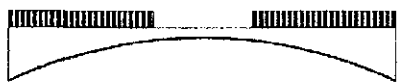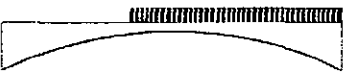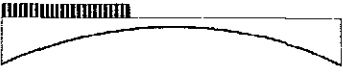Table 13   Load case 4: maximum positive moment at springing and maximum negative moment at quarter point, Frankford Avenue Bridge.

Location:	Left springing	Left quarter point
Axial force (kips)	-198	-169
Bending moment (k-ft)	-112	-6
Axial stress (psi)	-114	-173
Bending stress (psi)	-123	-21
Combined stress at intrados (psi)	-237	-194
Combined stress at extrados (psi)	9	-153

Table 14   Load case 5: maximum negative moment at springing and maximum positive moment at quarter point, Frankford Avenue Bridge.

Location:	Left springing	Left quarter point
Axial force (kips)	-177	-142
Bending moment (k-ft)	-272	35
Axial stress (psi)	-102	-146
Bending stress (psi)	-300	124
Combined stress at intrados (psi)	-402	-22
Combined stress at extrados (psi)	198	-269

2.2.4. Distribution of Axial Forces and Bending Moments

Table 15 lists the moments and axial forces in the concrete and steel for the loading conditions considered. Ratios of forces in the concrete and steel are nearly identical to the stiffness ratios at a particular arch section (see Tables 8 and 9). In general, at the springing, the concrete carries about 95 percent of the total axial force and about 91 percent of the total bending moment. At the crown, the concrete carries about 90 percent of the axial force and bending moment.

Table 15   Force distribution between concrete and steel, Frankford Avenue Bridge.

	Concrete	Steel	Ratio (C/S)
Load Case 1, Location: Springing (20)			
Axial force (kips)	-216	-10.9	19.8
Bending moment (k-ft)	-201	-19.6	10.3
Load Case 2, Location: Crown (1)			
Axial force (kips)	-150	-17.9	8.4
Bending moment (k-ft)	12	1.3	9.2
Load Case 3, Location: Crown (1)			
Axial force (kips)	-148	-17.6	8.4
Bending moment (k-ft)	-10	-1.1	9.1
Load Case 4, Location: Springing (20)			
Axial force (kips)	-198	-10	19.8
Bending moment (k-ft)	-112	-10.9	10.3
Load Case 4, Location: Quarter point (10)			
Axial force (kips)	-169	-15.2	11.1
Bending moment (k-ft)	-6	-0.68	8.8
Load Case 5, Location: Springing (20)			
Axial force (kips)	-177	-8.9	19.9
Bending moment (k-ft)	-272	-26.6	10.2
Load Case 5, Location: Quarter point (10)			
Axial force (kips)	-142	-12.8	11.1
Bending moment (k-ft)	35	4.1	8.5

2.3. Observations

The Frankford Avenue arch bridge over Poquessing Creek is very similar to closed-spandrel arches designed by the Concrete-Steel Engineering Co. Its reinforcement is essentially that patented by Von Emperger in 1897; it does not rely on bonding between concrete and steel to achieve composite behavior. The small stresses in both concrete and steel for various loading conditions indicate that the design procedure used was very conservative. The bridge is in all likelihood adequate for modern truck loads.

The Frankford Avenue Bridge is not innovative in the sense that it does not embody new developments in arch forms, reinforcing systems or engineering design methods. However, its exceptional performance and durability for over ninety years attest to the success of the design and to the quality of its construction.

3. CAMPBELL'S BRIDGE

3.1. Conceptual Design

Campbell's Bridge, built over Unami Creek in Milford Township, Bucks County, is shown schematically in Figure 15. It was constructed in 1906-07, approximately two years after the Frankford Avenue bridge, replacing a stone arch bridge washed away on 3 August 1906. It is an open-spandrel form with two fixed-fixed arches spanning 72'-0" (21.95 m). The position of the arch axis has been measured at only a few points, therefore its shape is uncertain. Localized spalling of the concrete cover has exposed some of the arch reinforcement. It appears that the principal arch reinforcement consists of six square deformed bars near the intrados and extrados, without lacing. The design thus depends on the bond between the reinforcement and the concrete, which is the "modern" conception of reinforced concrete. In contrast with the Frankford Avenue Bridge, the cast concrete is rougher, but the cost of Campbell's Bridge was significantly lower.

The intriguing question is why an open spandrel form was used. A speculation is that the form presents a more open profile for the exceptional stream flows that had destroyed the previous closed-spandrel stone arch. The design procedure used is unknown. From a modern viewpoint, the open-spandrel form introduces the issue of interaction between the arch, the cross beams and the reinforced concrete deck. The complexity of modeling the interaction strongly suggests that the designers simply used a model of the arch axis with gravity loads at the cross-beam locations. The actual structural behavior is much different, as indicated by modern structural analyses.

3.2. Structural Behavior

3.2.1. Geometry

Most of the significant dimensions of the bridge have been taken from an inspection report by the Commonwealth of Pennsylvania Department of Highways, dated 24 May 1932.[50] No original drawings from design or construction of the bridge have been located.[51] The shape of the arch was estimated from a field survey, performed by Erdman Anthony Associates in 1992, which gives the elevations above stream level at 9 points along the arch.[52] However with so few survey points, no definitive conclusion can be reached on the geometric shape of the arch. Both circular and parabolic arcs can be fit to the available 9 elevation points with nearly equal

---

[50] Bridge Inspection Report, 24 May 1932, on file at Commonwealth of Pennsylvania Department of Transportation, Saint Davids, Pennsylvania.

[51] U.S. Department of the Interior, Historic American Engineering Record (HAER), No. PA-451, "Campbell's Bridge," 1997, Prints and Photographs Division, Library of Congress, Washington, D.C.

[52] Erdman Anthony Associates, Inspection Report, 15 September 1992, on file at Commonwealth of Pennsylvania Department of Transportation, Saint Davids, Pennsylvania.

amounts of error. In addition, the relatively shallow arch (approximately a 7.5 span-to-rise ratio) makes the differences between circular and parabolic arcs very slight.

Polygonal or parabolic profiles are more appropriate structural forms for open-spandrel arches.[53] However, fabrication of formwork for a circular arch is simpler than for a parabolic arch. The analyses performed in this report assume a circular profile. It is expected that analyses with parabolic geometry would result in negligible differences.

Figure 15 shows several views of the bridge based on available drawings and field measurements.[54] Figure 16 shows the node and element numbering used for the computer models. Appendix C gives nodal coordinates and other details of the model. The focus of these analyses is to assess the contribution of the bridge deck in stiffening the arch.

3.2.2. Section Properties

Because the reinforcement consists of deformed square bars without lacing, the elements of Campbell's Bridge are defined with transformed section properties instead of parallel concrete and steel elements. A transformed section combines the properties of the concrete and steel based on the ratio, n, of elastic moduli. A modular ratio of 15 is assumed, based on a concrete modulus of 2,000 ksi and a steel modulus of 30,000 ksi.[55]

Currently, the reinforcing steel in the arch is exposed by spalling of the concrete cover at several locations. From field measurements the bars are estimated to be 3/4" deformed square bars. Deformations are one of the many methods used at the turn of the twentieth century to aid in mechanical bond between the steel and concrete.[56] At the intrados near the crown in the downstream arch, the concrete has spalled off across the full width of the arch and six equally spaced square bars are clearly visible. It is assumed that six additional bars are symmetrically placed along the extrados of the arch. No visible evidence was found of ties or stirrups holding the longitudinal steel in place, even in areas of spall several feet long. The concrete on the underside of the deck remains in sound condition with no exposed reinforcing steel, therefore the steel is assumed to be 3/4" bars spaced at 6" intervals at the top and bottom faces.

Table 16 lists the section properties (cross-sectional area and moment of inertia) for each arch section and for typical deck and vertical members. At the crown of the bridge the arch and deck become monolithic, and thus the section properties for Members 4 and 5 must include the stiffness of the combined cross section. The arch rib projects approximately 1'-9" (0.533 m) below the underside of the deck, as shown in Figure 15. Although the deck extends a total of 5'-11" (1.80 m) from the inside face of the arch rib to the centerline of the bridge, only a portion

---

[53] HAER No. IA-89, "Structural Study of Reinforced Concrete Arch Bridges."

[54] Field measurements by the authors on 24 July 1997.

[55] Turneaure and Maurer, ch. 10; Marsh, 81-82.

[56] HAER No. IA-89, "Structural Study of Reinforced Concrete Arch Bridges."

of the deck should be included in the calculation of section properties. Current concrete design codes recommend including a distance equal to the projection of the rib below the slab, which here equals 1'-9" (0.533 m).[57] Similarly, in the members where the deck is separate from the arch rib, a total width of 4'-9" (1.45 m) (3' width of rib plus 1'-9" projection) is used to calculate section properties. All analyses consider one arch rib and a tributary area of one-half the width of the bridge.

Table 16   Section properties, Campbell's Bridge.

Location	Member	Depth (in)	Area (in²)	Moment of inertia (in⁴)
Arch	1, 8	33.6	1,303	131,500
Arch	2, 7	29.5	1,155	89,800
Arch	3, 6	26.0	1,031	62,300
Arch & deck*	4, 5	24.3	2,350	558,000
Deck	9 to 14	22.2	1,640	104,200
Vertical	15 to 18	24.5	1,493	102,300

Note:

*   Members 4, 5 combine properties from arch ring and deck.

3.2.3. Dead and Live Loads

A concrete density of 150 pcf was assumed, accounting for both concrete and reinforcing steel. Dead loads of the arch and deck were applied as uniformly distributed loads. Point loads were added at the appropriate nodes to represent the dead loads of the cross beams. Appendix C lists the magnitudes of all loads for the model. A live load of 100 psf was assumed, and two load cases were considered, full-span and half-span. The 100 psf roadway live load was a typical late nineteenth-century design load for bridges located in rural areas. Because only eight members are necessary to define the arch, analysis for all of the load cases used for the Frankford Avenue Bridge is not deemed necessary. Instead, the live load on the full span (symmetric) produces maximum axial forces, while the live load on the half span (asymmetric) produces maximum bending moments. The live load is applied to the deck members as an uniformly distributed load of magnitude 0.77 kip/ft.

---

[57] American Concrete Institute, *ACI Standard 318-95: Building Code Requirements for Structural Concrete* (Farmington Hills, Michigan: American Concrete Institute, 1995), section 13.2.

3.2.4. Stress Analysis

Tables 17 and 18 give the results of the computer analyses.[58] For the live load applied across the whole span, the maximum compression of 368 kips in the arch occurs at the springing producing an axial compressive stress of 282 psi. A moment of 133 kip-ft also occurs at the springing, resulting in the maximum combined stress of 486 psi in compression. As noted for the Frankford Avenue Bridge, typical 28-day compressive strengths for concrete produced in the early twentieth century would have been in the range of 2,000 to 3,000 psi.[59] The maximum tensile stress in the arch segments was found to be 96 psi in member 3; and in the deck 165 psi in member 10. The tensile strength of the concrete would likely have been about 200 psi, and so only minor, if any, flexural cracking is likely to have occurred. Note that the axial force and moment in member 4, the monolithic section combining the arch and deck, are relatively large, yet due to the large bending and axial stiffnesses of this section, the stresses remain small. In general for a statically indeterminate structure, elements with large stiffnesses carry large forces.

For load case 2, maximum moments are produced in the arch and deck, but compressive and tensile stresses remain low. The maximum compressive stress of 488 psi occurs at the springing on the loaded side (member 1); and the maximum tensile stress of 175 psi, in the deck at member 10.

---

[58] Sign conventions:
Axial forces and stresses:
$+P$ = Tension
$-P$ = Compression
Bending moments:
$+M$ = Compression at extrados, tension at intrados
$-M$ = Tension at extrados, compression at intrados

[59] Turneaure and Maurer, ch. 2; Marsh, ch. 2.

Table 17   Load case 1: DL + LL (full span), Campbell's Bridge.

Member location:	1,8 Arch	2,7 Arch	3,6 Arch	4,5 Arch & deck
Axial force (kips)	-368	-271	-102	-327
Bending moment (k-ft)	133	108	-78	-261
Axial stress (psi)	-282	-235	-99	-139
Bending stress (psi)	203	213	-194	-52 / -72
Combined stress at extrados (psi)	-486	-447	96	54
Combined stress at intrados (psi)	-79	-22	-293	-211
Member location:	9,14 Deck	10,13 Deck	11,12 Deck	
Axial force (kips)	-5	-79	-229	
Bending moment (k-ft)	81	167	-114	
Axial stress (psi)	-3	-48	-139	
Bending stress (psi)	104	213	-146	
Combined stress at top (psi)	-107	-261	7	
Combined stress at bottom (psi)	100	165	-285	

Table 18   Load case 2: DL + LL (half span), Campbell's Bridge.

Member location:	1 Arch	2 Arch	3 Arch	4 Arch & deck
Axial force (kips)	-359	-259	-90	-301
Bending moment (k-ft)	139	109	-80	-256
Axial stress (psi)	-276	-224	-87	-128
Bending stress (psi)	213	215	-201	-51 / -71
Combined stress at extrados (psi)	-488	-439	113	61
Combined stress at intrados (psi)	-63	-10	-288	-199
Member location:	8 Arch	7 Arch	6 Arch	5 Arch & deck
Axial force (kips)	-321	-241	-97	-301
Bending moment (k-ft)	108	92	-61	-224
Axial stress (psi)	-246	-209	-94	-128
Bending stress (psi)	165	181	-153	-165 / -62
Combined stress at extrados (psi)	-412	-390	59	37
Combined stress at intrados (psi)	-81	-28	-247	-190

Table 18   (continued)

Member location:	9 Deck	10 Deck	11 Deck
Axial force (kips)	11.4	-66	-214
Bending moment (k-ft)	83	168	-118
Axial stress (psi)	7	-40	-130
Bending stress (psi)	106	215	-151
Combined stress at top (psi)	-99	-255	20
Combined stress at bottom (psi)	113	175	-281
Member location:	14 Deck	13 Deck	12 Deck
Axial force (kips)	-20	-80	-207
Bending moment (k-ft)	65	138	-94
Axial stress (psi)	-12	-49	-126
Bending stress (psi)	83	176	-120
Combined stress at top (psi)	-95	-225	-6
Combined stress at bottom (psi)	71	128	-246

3.3.   Effect of Deck Stiffening

Tables 19 and 20 compare member forces from analyses including and excluding the deck. The analysis excluding the deck uses equivalent nodal loads to apply the dead and live loads directly to the arch. For both load cases, including the deck in the analysis substantially reduces the moments that the arch itself must carry. This reduction is most pronounced at the springing where the moment in the deck-stiffened analysis is approximately half that in the arch-only analysis. Member 4 near the crown, combining the arch and deck, carries greater moment in the deck-stiffened analysis, yet the large axial and bending stiffness of this section will still result in relatively small stresses. Figure 18 compares moment diagrams for load case 2 from the deck-stiffened model and the arch-only model. Again the deck provides a stiffening effect to the arch which reduces the moments at the springing.

Table 19   Load case 1: DL + LL (full span), Campbell's Bridge.

Member location:	1,8 Arch	2,7 Arch	3,6 Arch	4,5 Arch & deck
Analysis with arch & deck				
Axial force (kips)	-368	-271	-102	-327
Bending moment (k-ft)	133	108	-78	-261
Analysis with arch ring only				
Axial force (kips)	-379	-357	-342	-336
Bending moment (k-ft)	230	90	-98.6	-122

Table 20   Load case 2: DL + LL (half span), Campbell's Bridge.

Member location:	1 Arch	2 Arch	3 Arch	4 Arch & deck
Analysis with arch & deck				
Axial force (kips)	-359	-259	-90	-301
Bending moment (k-ft)	139	109	-80	-256
Analysis with arch ring only				
Axial force (kips)	-353	-330	-316	-309
Bending moment (k-ft)	285	102	-123	-123

3.4.   Observations

Campbell's Bridge is an early example of the open-spandrel form, which became dominant in the 1920s and 1930s. Its reinforcement is "modern," in the sense it relies on the bond between the steel and the concrete to achieve composite behavior, unlike the latticed reinforcement of the Frankford Avenue Bridge. Modern analyses indicate that the actual behavior of the bridge is that of a deck-stiffened arch. However, it is very likely that the model used for design was that of a simple arch with gravity loads at the locations of the cross-beams. Such a model is conservative. Even if the bridge did behave as two simple arches, the stresses in the concrete arches are predicted to be much smaller than the actual strength of the concrete.

Campbell's Bridge is very narrow (about fifteen feet wide), with no architectural detailing. Its design and execution seem to have been determined by strictly utilitarian, engineering and economic criteria. There is extensive spalling, which requires rehabilitation.

The spalling may be due to poor construction practices, insufficient concrete cover over the steel (it is generally much smaller than the 3-inch cover prescribed for the Frankford Avenue Bridge) or inadequate maintenance.

SOURCES CONSULTED

American Concrete Institute. *ACI Standard 318-95: Building Code Requirements for Structural Concrete.* Farmington Hills, Michigan: American Concrete Institute, 1995.

Bridge Inspection Report, 24 May 1932. On file at Commonwealth of Pennsylvania Department of Transportation, Saint Davids, Pennsylvania.

City of Philadelphia and Bucks County. "Specifications for the Construction of a Concrete Steel Arch Bridge on the Line of Frankford Avenue, over Poquessing Creek" (1903).

Cooper, T. "American Railroad Bridges." *Transactions of the American Society of Civil Engineers* 21 (1889): 1-54.

Cullmann, K. "Der Bau der Hölzener Brücken in den Vereinigen Staaten von Nordamerika." *Allgemeine Bauzeitung mit Abbildungen* (Vienna, Austria) 16 (1851): 69-129.

Doyne, W. T., and Blood, W. B. "An Investigation of the Strains Upon the Diagonals of Lattice Beams, with the Resulting Formulae." *ICE Proceedings* 11 (1851): 31-14.

Dreicer, G. K. "The Long Span: Intercultural Exchange in Building Technology." Ph.D. diss., Cornell University, May 1993.

Emperger, F. von. "Vault for Ceilings, Bridges, etc." U.S. Patent No. 583,464 (1897).

Erdman Anthony Associates. Bridge Inspection Report, 15 September 1992. On file at Commonwealth of Pennsylvania Department of Transportation, Saint Davids, Pennsylvania.

Gasparini, Dario, and Simmons, David. "American Truss Bridge Connections in the Nineteenth Century, Parts 1 and II." *Journal of Performance of Constructed Facilites* 11, No. 3 (1997): 119-29, 130-40.

Ghali, A., and Neville, A. M. *Structural Analysis.* London: Chapman and Hall, 1989.

Gray, G. E. "Notes on Early Practice in Bridge Building." *Transactions of the American Society of Civil Engineers* 37 (1897): 1-16.

James, J. G. "The Evolution of Iron Bridge Trusses to 1850." *Transactions of the Newcomen Society* 52 (1980-81): 67-101.

_____. "The Evolution of Wooden Bridge Trusses to 1850." *Journal of the Institute of Wood Science* 9 (June 1982): 116-35; (December 1982): 168-93.

Johnson, J. B., C. W. Bryan, and F. E. Turneaure. *The Theory and Practice of Modern Framed Structures,* 9th ed. New York: John Wiley and Sons, 1914.

Marsh, C. F. *A Concise Treatise on Reinforced Concrete.* New York: Van Nostrand, 1910.

Merriman, M., and H. S. Jacoby. *Roofs and Bridges.* 5th ed. New York: John Wiley and Sons, 1920.

_____. *Roofs and Bridges.* 6th ed. New York: John Wiley and Sons, 1922.

Snow, J. P. "Report of AREA Committee XV on Iron and Steel Structures." *Proceedings, Sixth Annual Convention of the AREA.* Chicago: American Railway Engineering Association, 1905.

Stowell, C. F., ed. "Strains on Railroad Bridges of the State." *Report of the Board of Commissioners of the State of New York.* Albany: Weed, Parsons & Co., 1891.

Thacher, E. "Concrete and Concrete-Steel in the United States." *Transactions of the American Society of Civil Engineers* 54, pt. E (1905).

Thomson, G. H. "American Bridge Failures." *Engineering* 46 (14 September 1888): 252-83.

Timoshenko, S., and G. H. MacCullough. *Elements of Strength of Materials.* 3rd ed. New York: Van Nostrand, 1949.

Turneaure, F. E., and E. R. Maurer. *Principles of Reinforced Concrete Construction.* 4th ed. New York: John Wiley and Sons, 1932.

U.S. Department of the Interior, Historic American Engineering Record (HAER) No. IA-89, "Structural Study of Reinforced Concrete Arch Bridges," 1997. Prints and Photographs Division, Library of Congress, Washington, D.C.

_____, HAER No. PA-451, "Campbell's Bridge," 1997. Prints and Photographs Division, Library of Congress, Washington, D.C.

_____, HAER No. PA-460, "Upper Bridge at Slate Run," 1997. Prints and Photographs Division, Library of Congress, Washington, D.C.

Vose, G. L. *Manual for Railroad Engineers and Engineering Students.* Boston: Lee and Shepard, 1878.

Withey, M. O., and J. Aston. *Johnson's Materials of Construction.* 5th ed. New York: John Wiley and Sons, 1919.

Figure 1. Canestota Station Bridge. Illustration from G. L. Vose, *Manual for Railroad Engineers and Engineering Students* (Boston: Lee and Shepard, 1878).
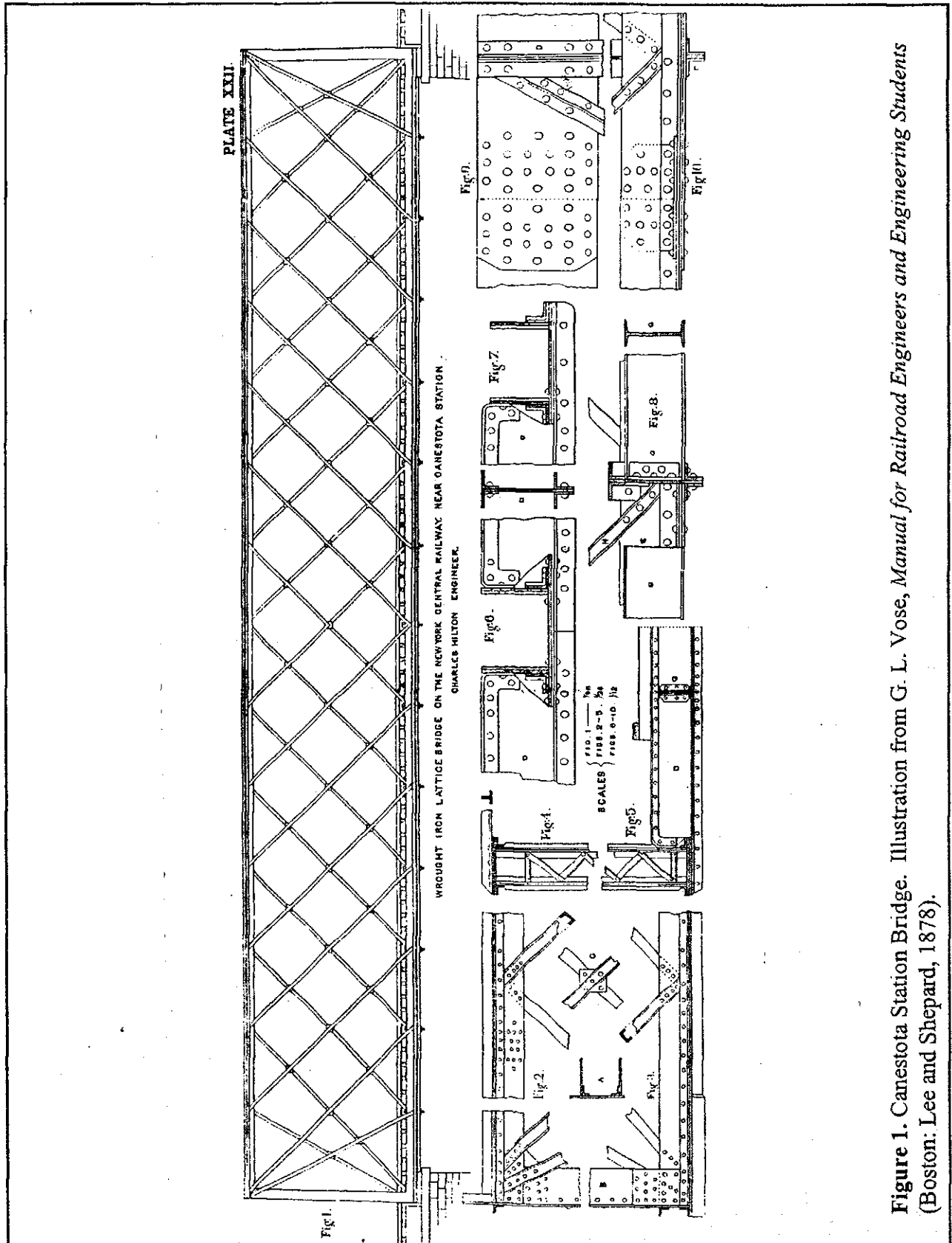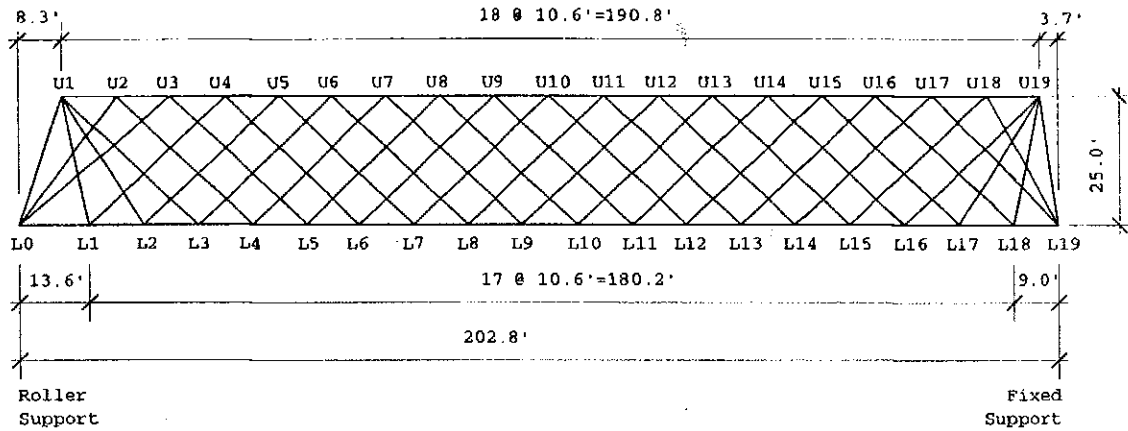
Figure 2. Elevation of lattice truss, Upper Bridge at Slate Run.
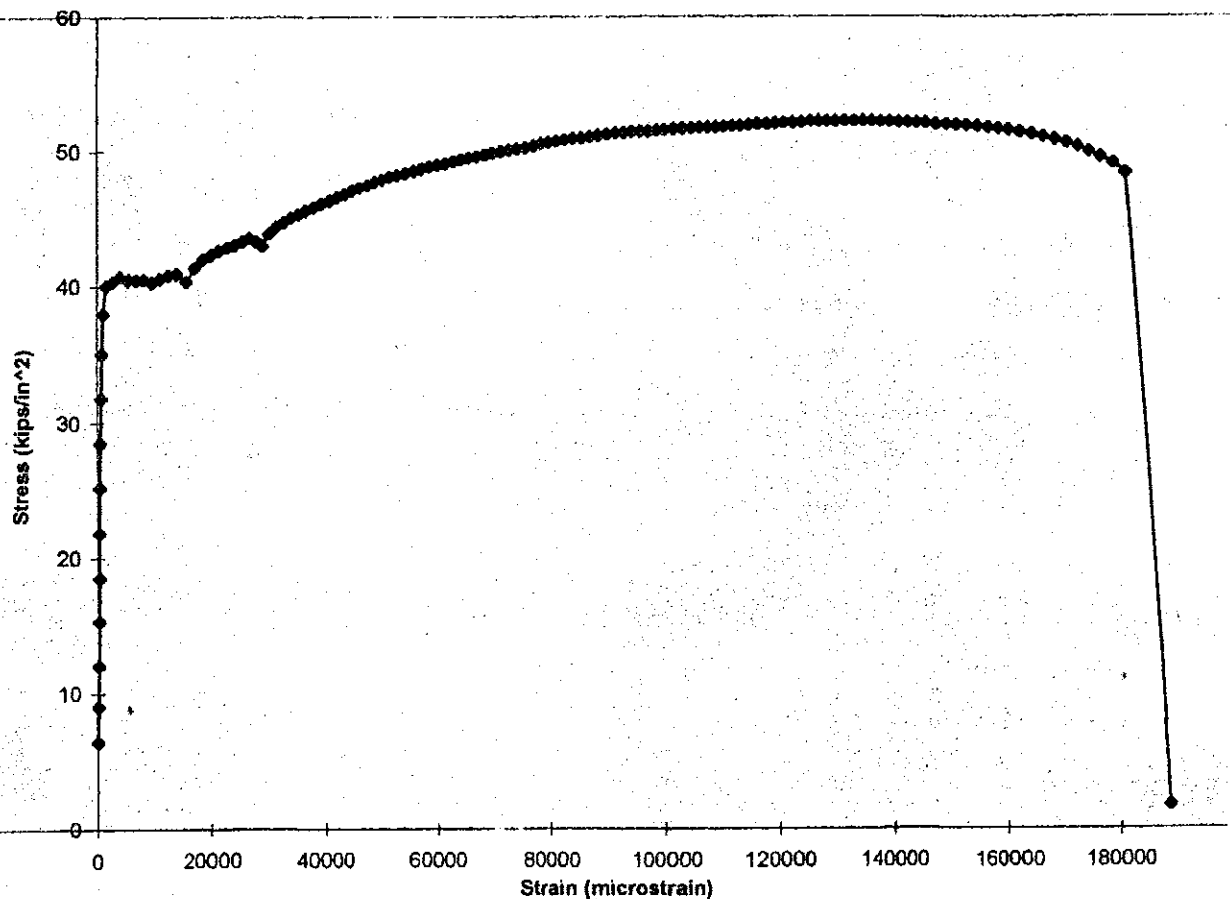
Figure 3. Uniaxial stress-strain curve for metal specimen found at site of Upper Bridge at Slate Run.
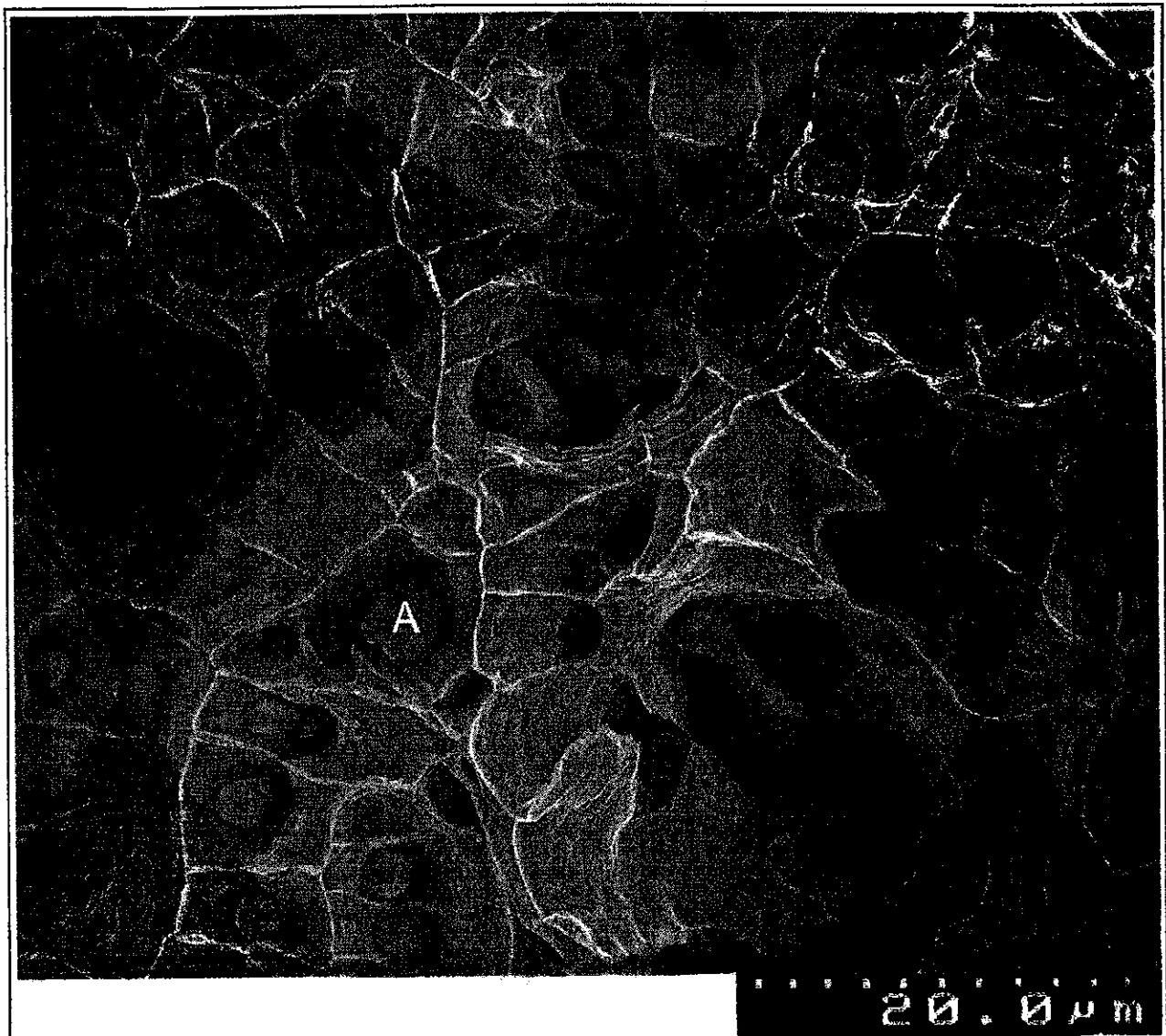
Figure 4. Fracture surface for metal specimen found at site of Upper Bridge at Slate Run.

Top Lateral
Bracing

Upper
Chord

Diagonals

Lower
Chord

Floor Beam

Diagonal
Strut

$N=0.2$ k (Compression)

$h=25'$

$R=7.6$ k

$w=80$ psf

$N=0.2$ k
(Tension)

$e \approx 8"$
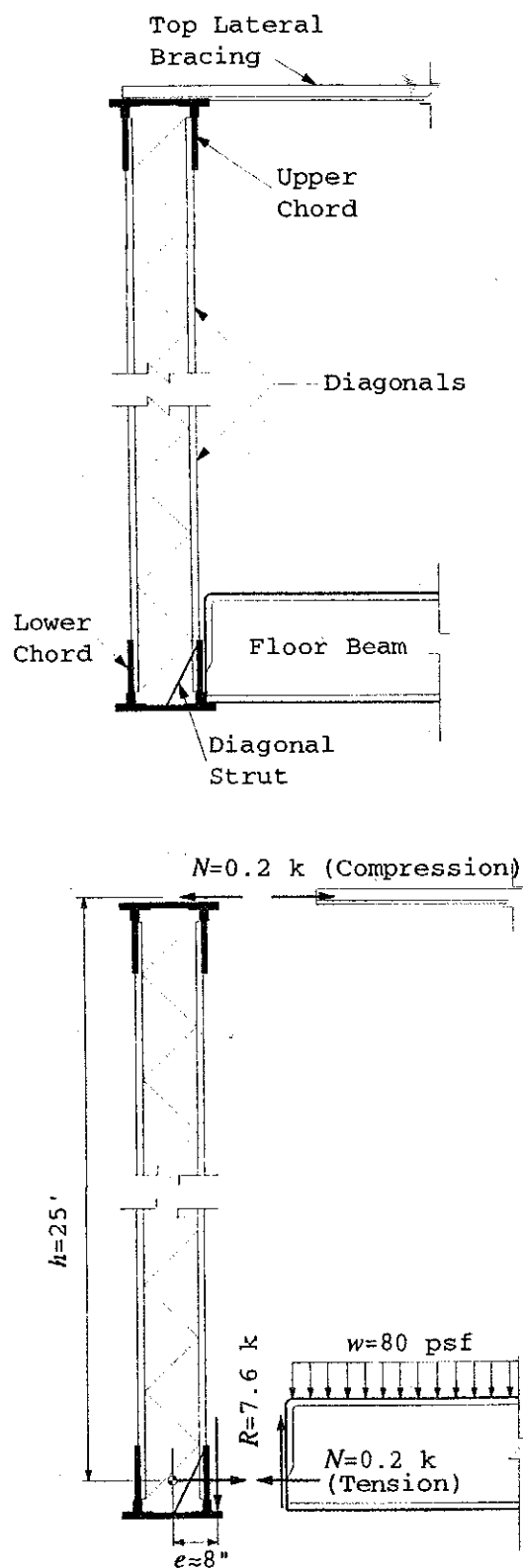
Figure 5. Floor beam to lower chord connection, Upper Bridge at Slate Run.
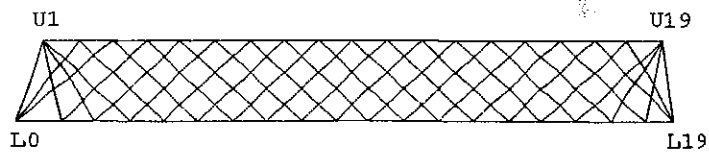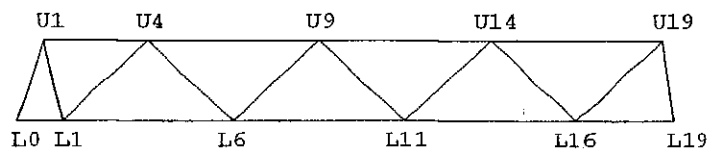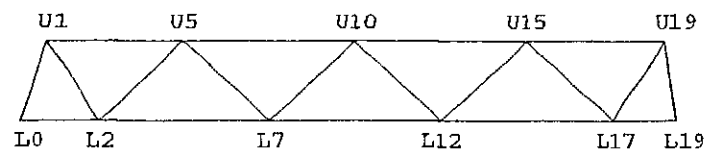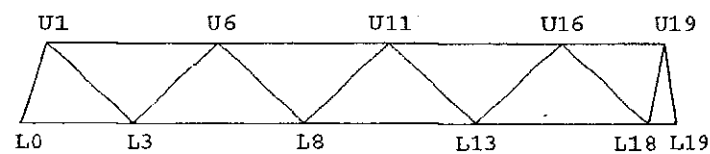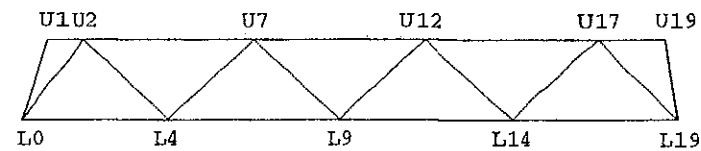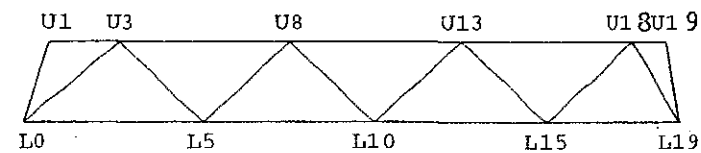
Figure 6. Lattice truss and component trusses, Upper Bridge at Slate Run.
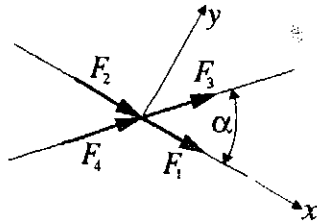
Figure 7. Axial forces in intersecting diagonals.

Some force transferred
to Truss 2 through
upper chord.
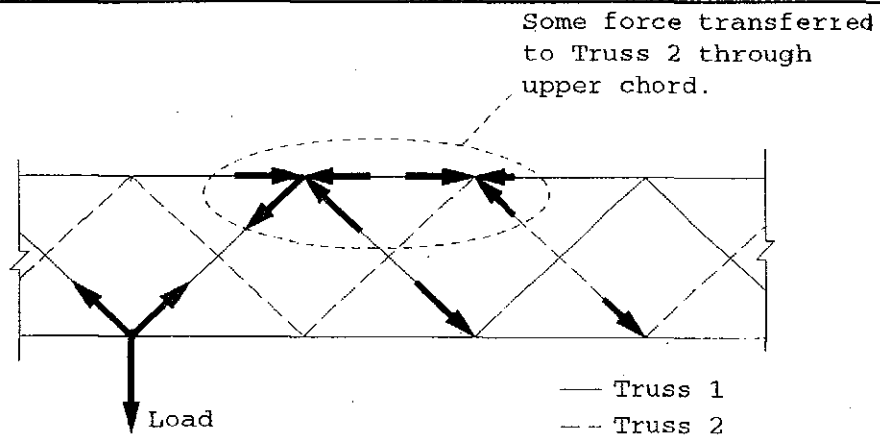
Load

—— Truss 1

— — Truss 2

Note: Some member forces
not shown for clarity.

Figure 8. Interaction of trusses through chord.
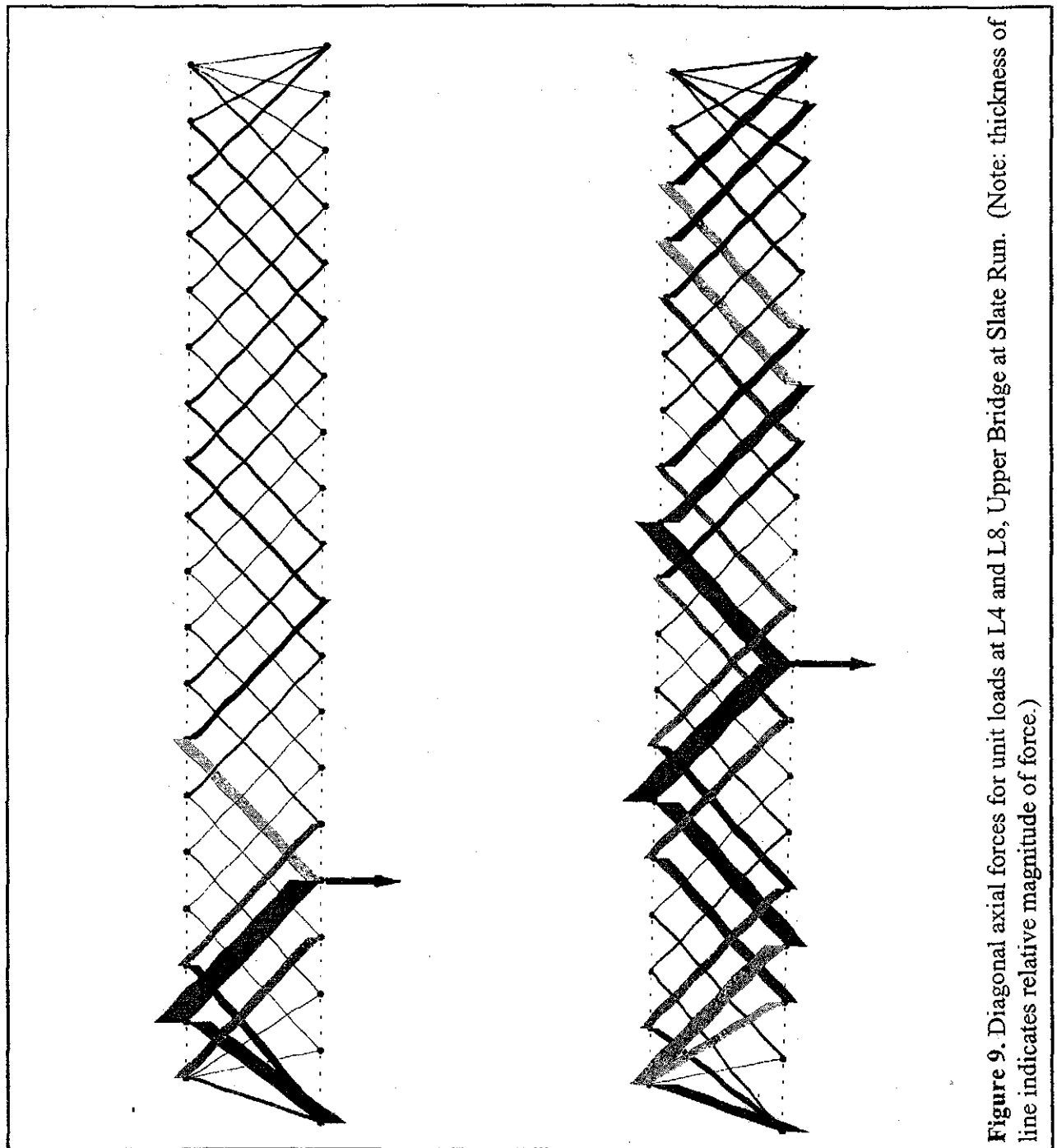
Figure 9. Diagonal axial forces for unit loads at L4 and L8, Upper Bridge at Slate Run. (Note: thickness of line indicates relative magnitude of force.)
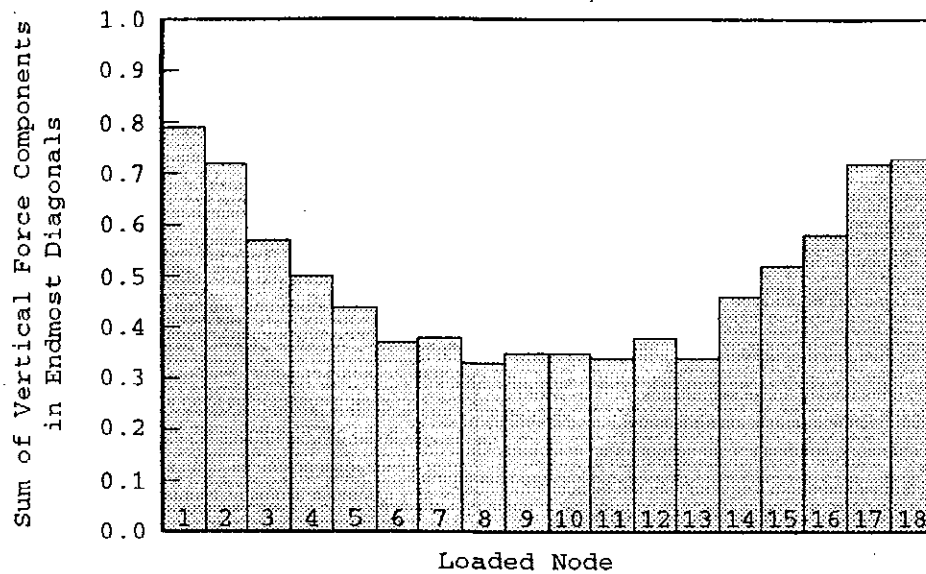
Figure 10. Interaction of component trusses, Upper Bridge at Slate Run.

Figure 11. Typical axial force distributions under dead load and roadway live load, Upper Bridge at Slate Run. (Note: thickness of line indicates relative magnitude of force.)
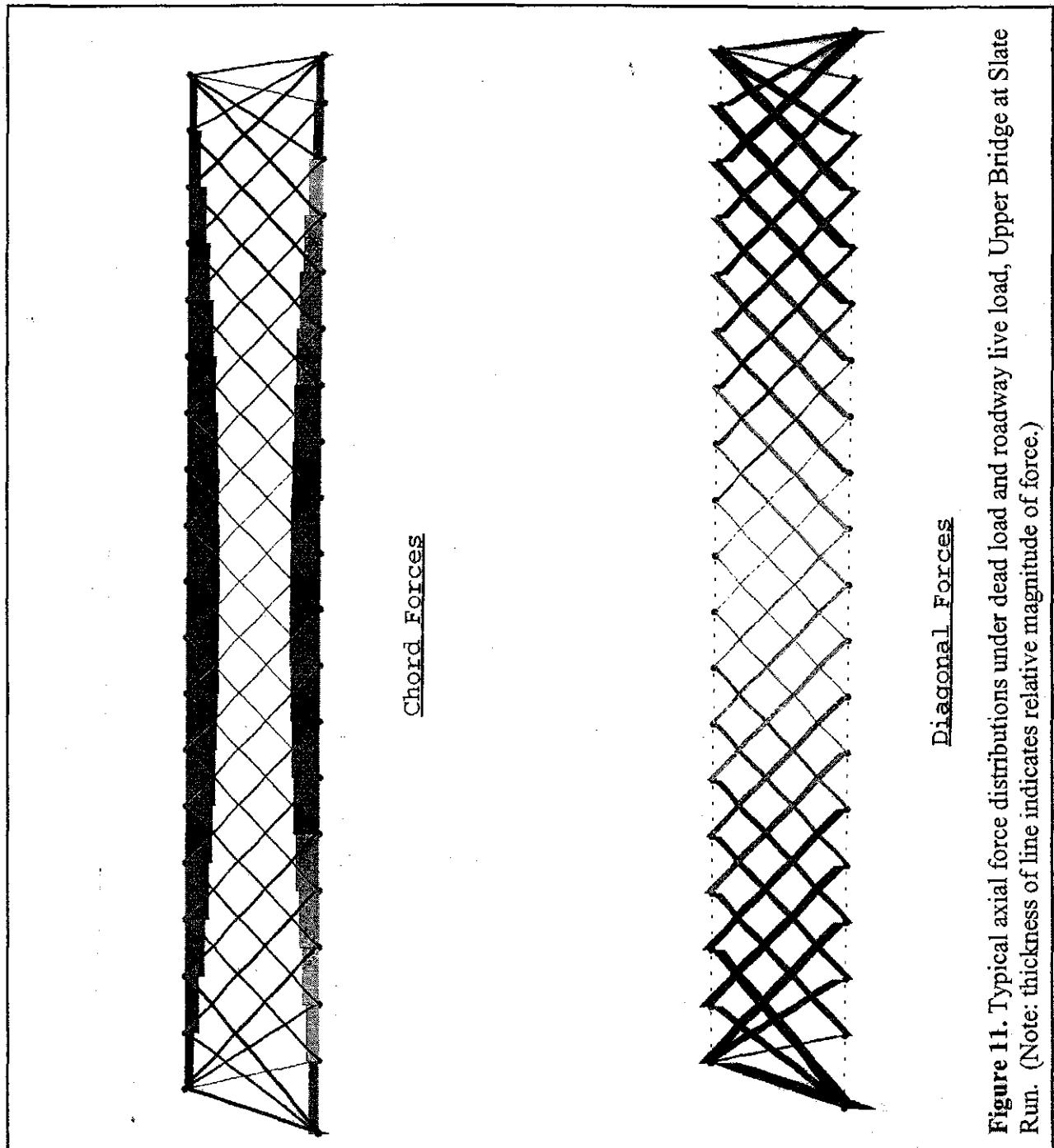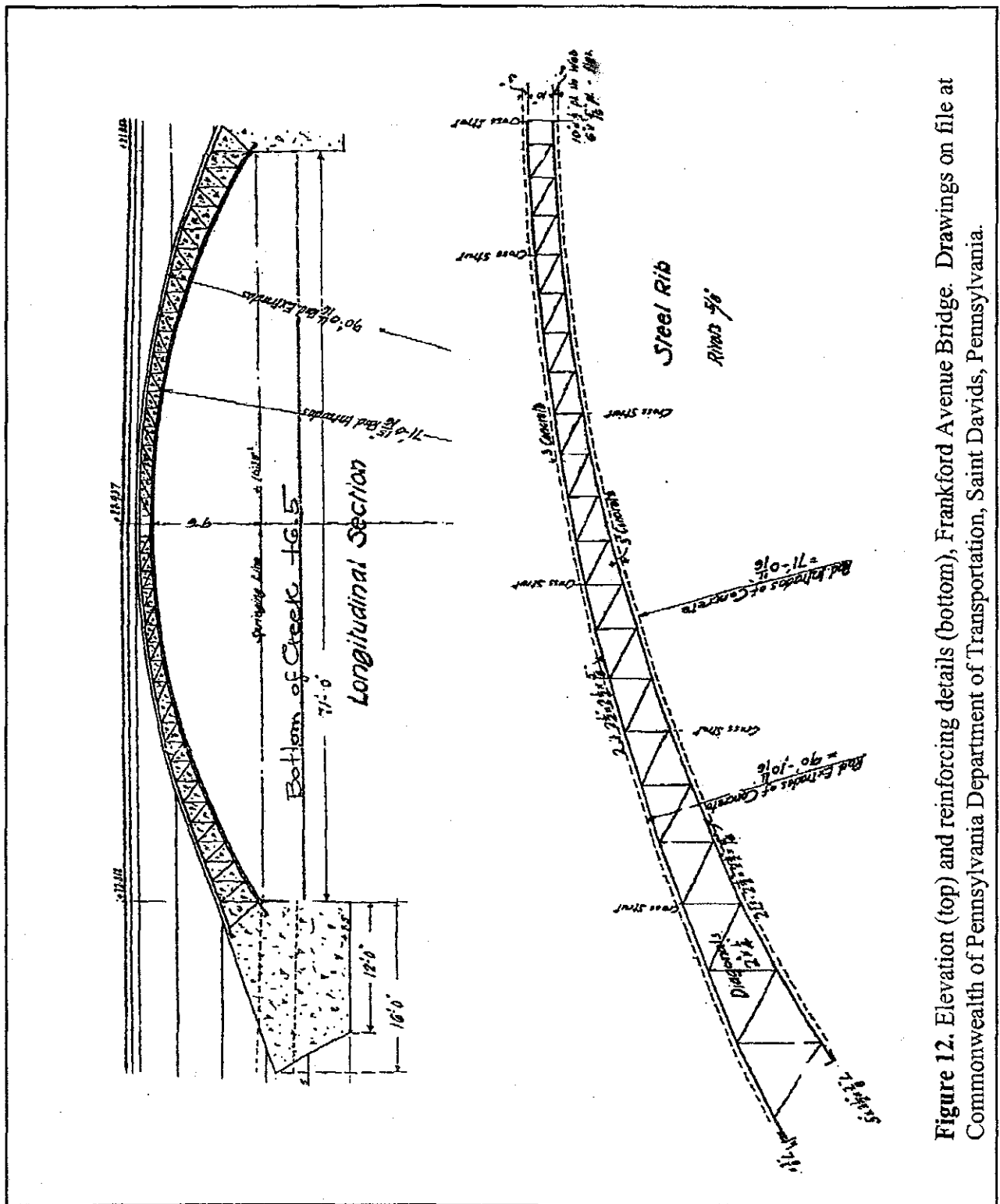
Figure 12. Elevation (top) and reinforcing details (bottom), Frankford Avenue Bridge. Drawings on file at Commonwealth of Pennsylvania Department of Transportation, Saint Davids, Pennsylvania.
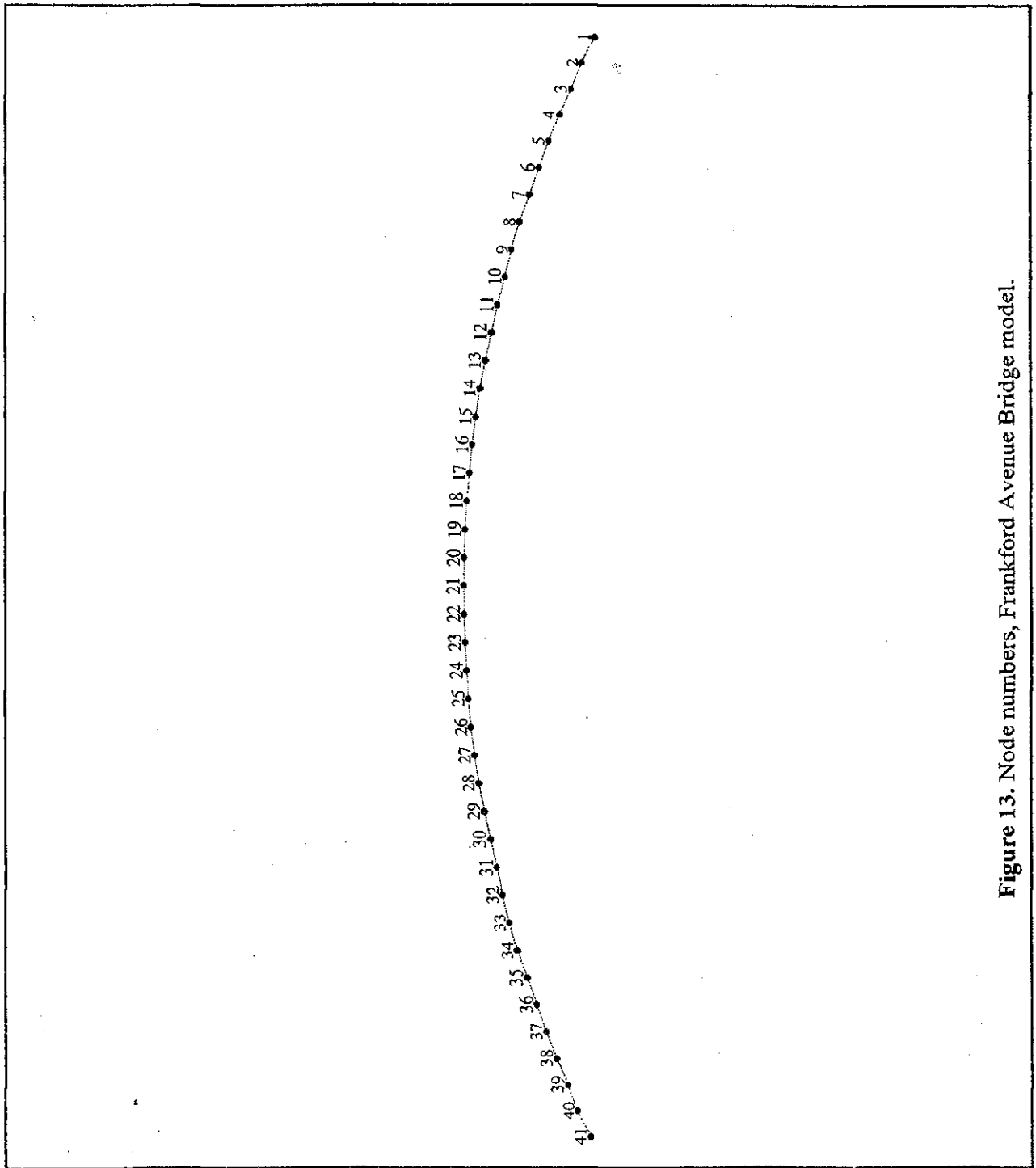
Figure 13. Node numbers, Frankford Avenue Bridge model.

-135 k

-177 k   -170 k

-8 k-ft

-136 k-ft

-272 k-ft
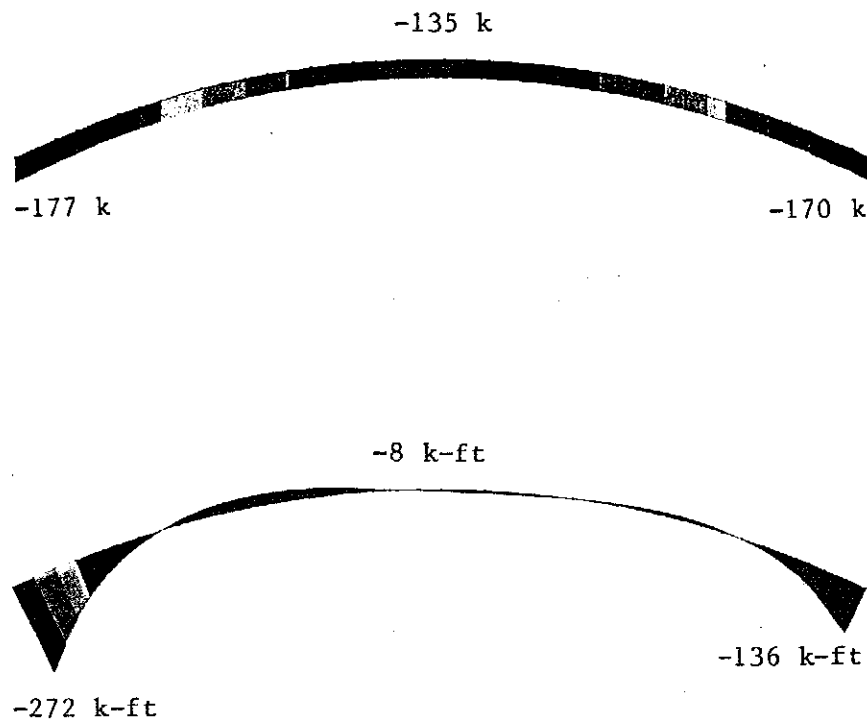
Figure 14. Axial force (top) and bending moment (bottom) diagrams for load case 5, Frankford Avenue Bridge. (Note: thickness of line indicates relative magnitude of force or bending moment.)

Section C

Section B   Section A

16-3 5/8"

10'-0"   10'-0"   10'-0"   6'-0" 4'-0'

Plan

C   B   A

9'-6"

72'-0"

3'-0"

Extrados
R 83'-5 1/2"

Intrados
R 73'-3 1/2"

Elevation And Section
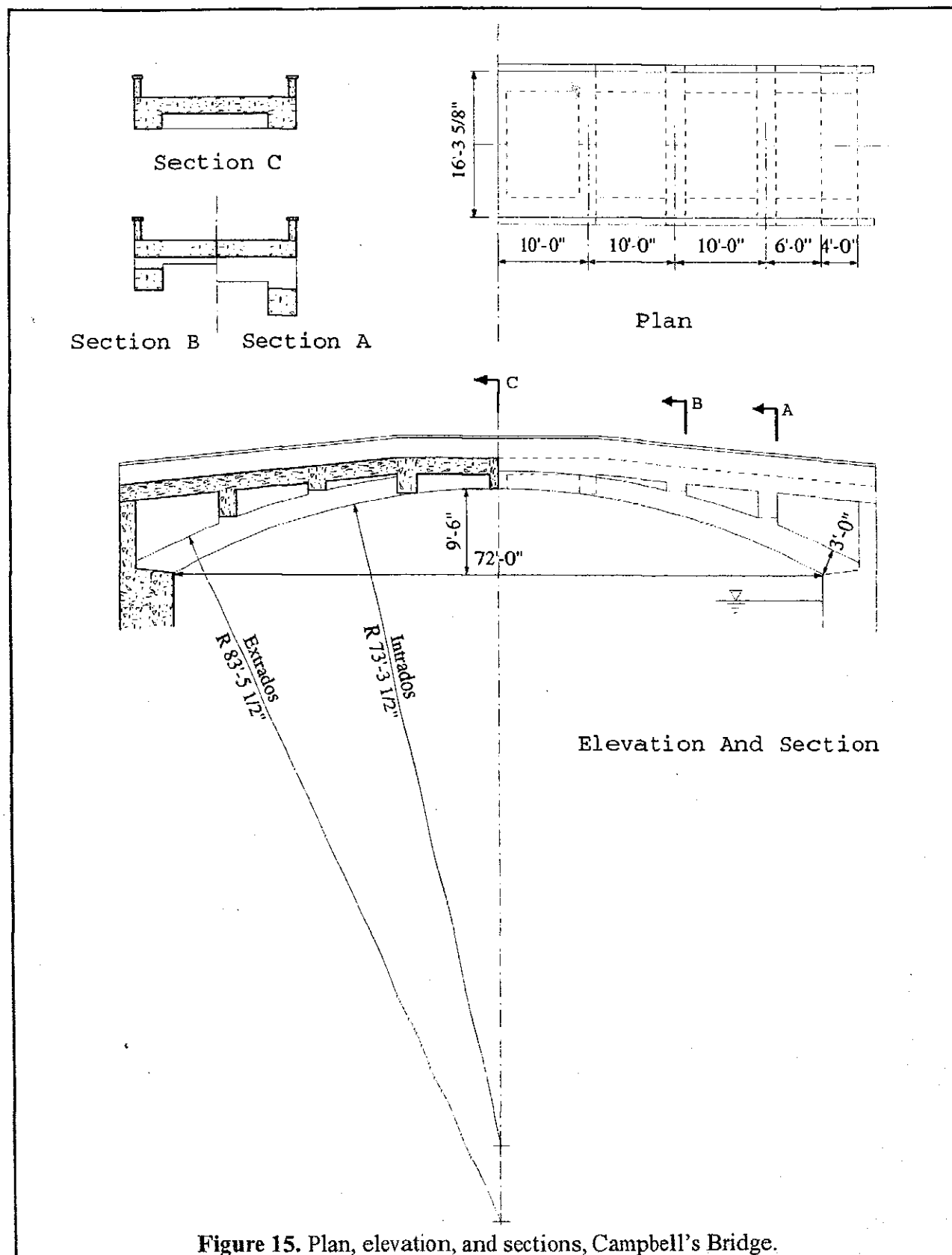
Figure 15. Plan, elevation, and sections, Campbell's Bridge.
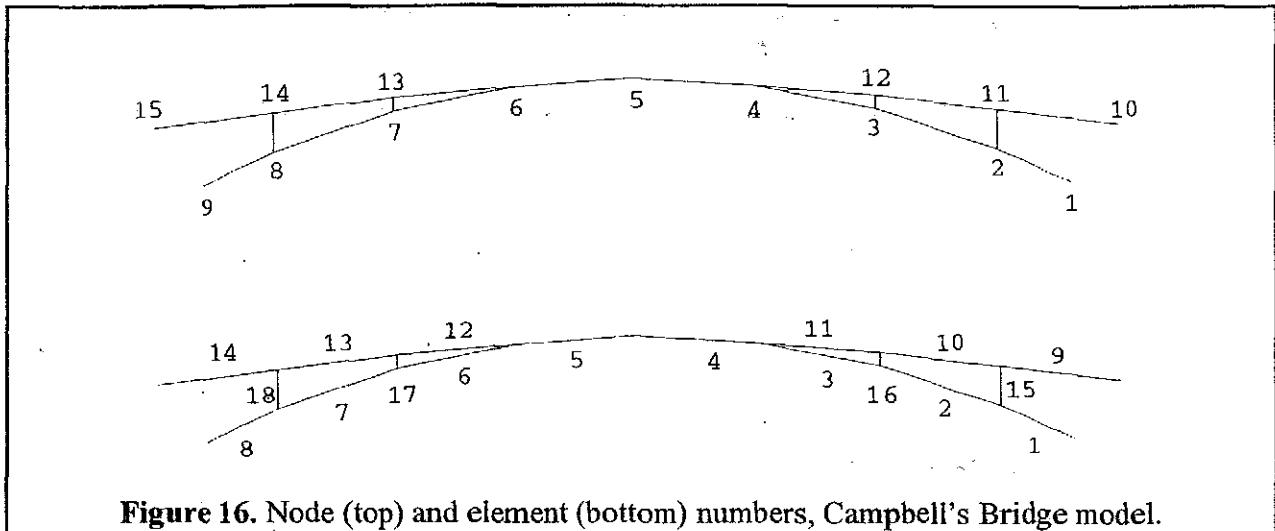
Figure 16. Node (top) and element (bottom) numbers, Campbell's Bridge model.
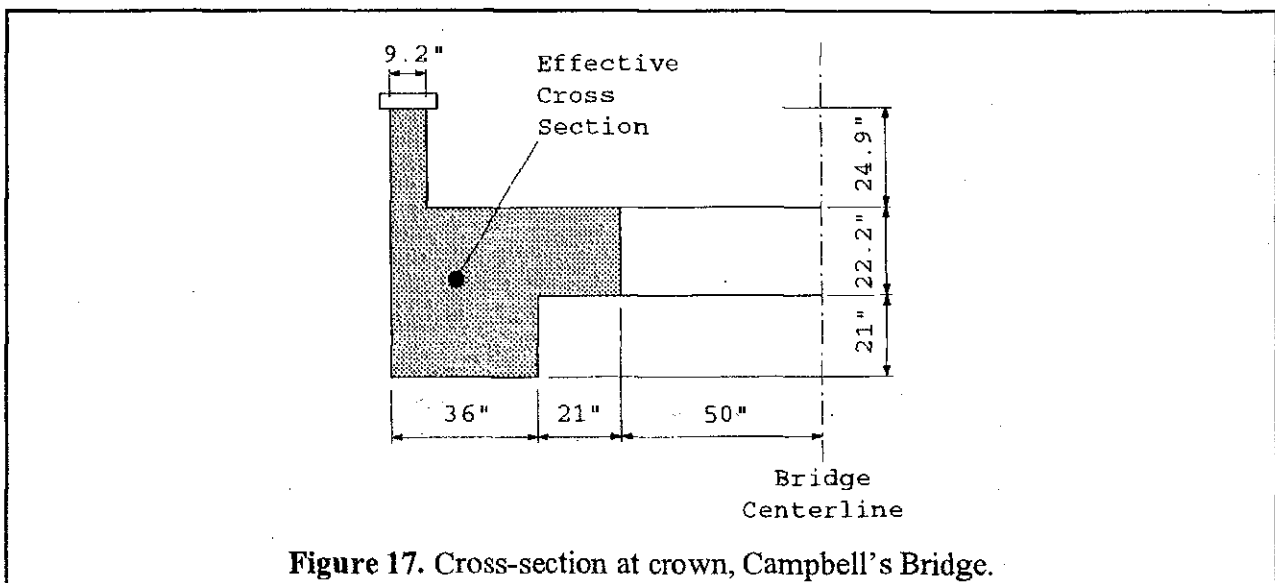
Figure 17. Cross-section at crown, Campbell's Bridge.
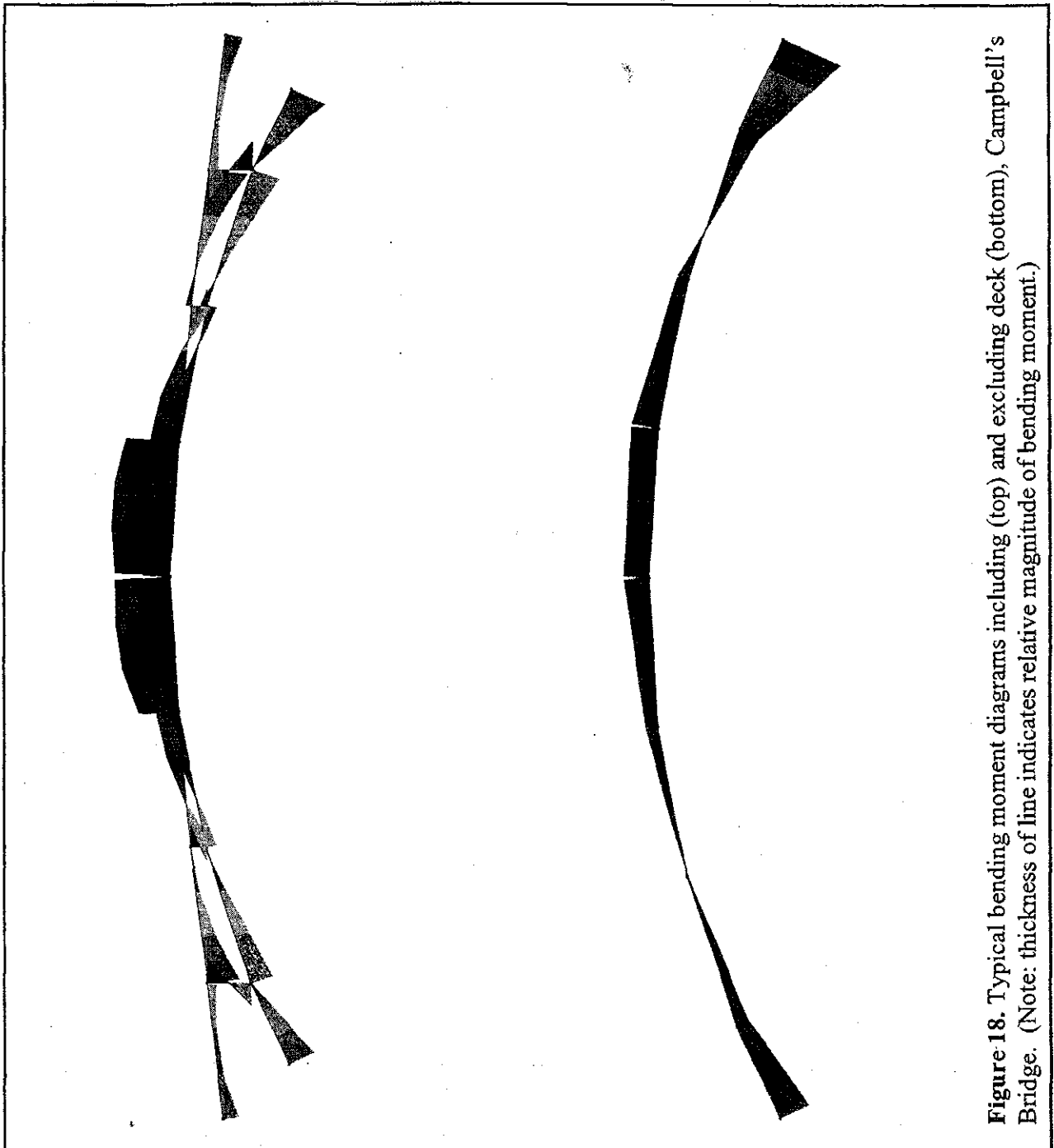
Figure 18. Typical bending moment diagrams including (top) and excluding deck (bottom), Campbell's Bridge. (Note: thickness of line indicates relative magnitude of bending moment.)

APPENDIX A: Upper Bridge at Slate Run Structural Model Definition

Table A-1　　　　Nodal coordinates.

Panel point	Joint No.	X coordinate (ft)	Y coordinate (ft)	Panel point	Joint No.	X coordinate (ft)	Y coordinate (ft)
L0	1	0.0	0.0	U1	21	8.3	25.0
L1	2	13.6	0.0	U2	22	18.9	25.0
L2	3	24.2	0.0	U3	23	29.5	25.0
L3	4	34.8	0.0	U4	24	40.1	25.0
L4	5	45.4	0.0	U5	25	50.7	25.0
L5	6	56.0	0.0	U6	26	61.3	25.0
L6	7	66.6	0.0	U7	27	71.9	25.0
L7	8	77.2	0.0	U8	28	82.5	25.0
L8	9	87.8	0.0	U9	29	93.1	25.0
L9	10	98.4	0.0	U10	30	103.7	25.0
L10	11	109.0	0.0	U11	31	114.3	25.0
L11	12	119.6	0.0	U12	32	124.9	25.0
L12	13	130.2	0.0	U13	33	135.5	25.0
L13	14	140.8	0.0	U14	34	146.1	25.0
L14	15	151.4	0.0	U15	35	156.7	25.0
L15	16	162.0	0.0	U16	36	167.3	25.0
L16	17	172.6	0.0	U17	37	177.9	25.0
L17	18	183.2	0.0	U18	38	188.5	25.0
L18	19	193.8	0.0	U19	39	199.1	25.0
L19	20	202.8	0.0				

Table A-2　　　　Member definitions.

Member No.	Joint 1	Joint 2	Section No.	Section type	Member No.	Joint 1	Joint 2	Section No.	Section type
1	1	2	7	LC-1	10	10	11	11	LC-5
2	2	3	7	LC-1	11	11	12	11	LC-5
3	3	4	7	LC-1	12	12	13	11	LC-5
4	4	5	8	LC-2	13	13	14	10	LC-4
5	5	6	9	LC-3	14	14	15	10	LC-4
6	6	7	10	LC-4	15	15	16	9	LC-3
7	7	8	10	LC-4	16	16	17	12	LC-6
8	8	9	11	LC-5	17	17	18	7	LC-1
9	9	10	11	LC-5	18	18	19	7	LC-1

Table A-2 (continued)

Member No.	Joint 1	Joint 2	Section No.	Section type	Member No.	Joint 1	Joint 2	Section No.	Section type
19	19	20	7	LC-1	93	11	33	22	TD-4
20	21	22	1	UC-1	98	12	34	22	TD-4
21	22	23	1	UC-1	103	13	35	22	TD-4
22	23	24	2	UC-2	108	14	36	22	TD-4
23	24	25	3	UC-3	113	15	37	19	TD-3
24	25	26	4	UC-4	118	16	38	17	TD-2
25	26	27	5	UC-5	123	17	39	15	TD-1
26	27	28	6	UC-6	128	18	39	15	TD-1
27	28	29	6	UC-6	132	19	39	15	TD-1
28	29	30	6	UC-6	135	2	21	15	TD-1
29	30	31	6	UC-6	138	3	21	15	TD-1
30	31	32	6	UC-6	142	4	21	15	TD-1
31	32	33	6	UC-6	147	5	22	17	TD-2
32	33	34	5	UC-5	152	6	23	19	TD-3
33	34	35	4	UC-4	157	7	24	22	TD-4
34	35	36	3	UC-3	162	8	25	22	TD-4
35	36	37	2	UC-2	167	9	26	22	TD-4
36	37	38	1	UC-1	172	10	27	22	TD-4
37	38	39	1	UC-1	177	11	28	22	TD-4
38	1	21	13	EP	182	12	29	21	CD-5
39	1	22	14	CD-1	187	13	30	21	CD-5
43	1	23	14	CD-1	192	14	31	21	CD-5
48	2	24	16	CD-2	197	15	32	21	CD-5
53	3	25	18	CD-3	202	16	33	21	CD-5
58	4	26	20	CD-4	207	17	34	20	CD-4
63	5	27	21	CD-5	212	18	35	18	CD-3
68	6	28	21	CD-5	217	19	36	16	CD-2
73	7	29	21	CD-5	222	20	37	14	CD-1
78	8	30	21	CD-5	227	20	38	14	CD-1
83	9	31	21	CD-5	231	20	39	13	EP
88	10	32	22	TD-4					

Table A-3   Section properties.

Section No.	Section type	Weight (lb/ft)	Area (in²)	Moments of inertia Out-of-plane (in⁴)	Moments of inertia In-plane (in⁴)
1	UC-1	83	24.25	1,552	539
2	UC-2	101	29.75	1,785	659
3	UC-3	120	35.25	2,007	785
4	UC-4	139	40.75	2,228	887
5	UC-5	153	44.875	2,395	954
6	UC-6	176	51.75	2,672	1,054
7	LC-1	83	24.25	1,552	539
8	LC-2	112	33	1,988	739
9	LC-3	120	35.25	2,007	785
10	LC-4	139	40.75	2,228	887
11	LC-5	157	46.25	2,450	975
12	LC-6	101	29.75	1,785	659
13	EP	101	29.75	1,774	708
14	CD-1	29	8.436	362	13.69
15	TD-1	19	5.523	465	5.809
16	CD-2	19	5.633	225	5.877
17	TD-2	19	5.633	477	5.877
18	CD-3	16	4.781	196	5.109
19	TD-3	16	4.781	399	5.109
20	CD-4	19	5.5	226	4.433
21	CD-5	14	4.219	177	3.519
22	TD-4	14	4.219	344	3.519

APPENDIX B: Frankford Avenue Bridge Structural Model Definition

Table B-1   Nodal coordinates.

Node No.	X coordinate (ft)	Y coordinate (ft)	Node No.	X coordinate (ft)	Y coordinate (ft)
1	35.500	-8.197	22	-1.837	-0.021
2	33.840	-7.410	23	-3.674	-0.083
3	32.162	-6.661	24	-5.508	-0.188
4	30.467	-5.950	25	-7.340	-0.333
5	28.757	-5.278	26	-9.167	-0.521
6	27.032	-4.645	27	-10.991	-0.749
7	25.293	-4.052	28	-12.808	-1.019
8	23.542	-3.498	29	-14.619	-1.331
9	21.778	-2.983	30	-16.422	-1.683
10	20.002	-2.509	31	-18.217	-2.076
11	18.217	-2.076	32	-20.002	-2.509
12	16.422	-1.683	33	-21.778	-2.983
13	14.619	-1.331	34	-23.542	-3.498
14	12.808	-1.019	35	-25.293	-4.052
15	10.991	-0.749	36	-27.032	-4.645
16	9.167	-0.521	37	-28.757	-5.278
17	7.340	-0.333	38	-30.467	-5.950
18	5.508	-0.188	39	-32.162	-6.661
19	3.674	-0.083	40	-33.840	-7.410
20	1.837	-0.021	41	-35.500	-8.197
21	0.000	0.000			

Table B-2   Member definitions.

Member No.	Joint 1	Joint 2	Section No.	Material type	Member No.	Joint 1	Joint 2	Section No.	Material type
1	21	20	1	Conc.	9	13	12	9	Conc.
2	20	19	2	Conc.	10	12	11	10	Conc.
3	19	18	3	Conc.	11	11	10	11	Conc.
4	18	17	4	Conc.	12	10	9	12	Conc.
5	17	16	5	Conc.	13	9	8	13	Conc.
6	16	15	6	Conc.	14	8	7	14	Conc.
7	15	14	7	Conc.	15	7	6	15	Conc.
8	14	13	8	Conc.	16	6	5	16	Conc.

Table B-2 (continued)

Member No.	Joint 1	Joint 2	Section No.	Material type	Member No.	Joint 1	Joint 2	Section No.	Material type
17	5	4	17	Conc.	49	29	30	9	Conc.
18	4	3	18	Conc.	50	30	31	10	Conc.
19	3	2	19	Conc.	51	31	32	11	Conc.
20	2	1	20	Conc.	52	32	33	12	Conc.
21	21	20	21	Steel	53	33	34	13	Conc.
22	20	19	22	Steel	54	34	35	14	Conc.
23	19	18	23	Steel	55	35	36	15	Conc.
24	18	17	24	Steel	56	36	37	16	Conc.
25	17	16	25	Steel	57	37	38	17	Conc.
26	16	15	26	Steel	58	38	39	18	Conc.
27	15	14	27	Steel	59	39	40	19	Conc.
28	14	13	28	Steel	60	40	41	20	Conc.
29	13	12	29	Steel	61	21	22	21	Steel
30	12	11	30	Steel	62	22	23	22	Steel
31	11	10	31	Steel	63	23	24	23	Steel
32	10	9	32	Steel	64	24	25	24	Steel
33	9	8	33	Steel	65	25	26	25	Steel
34	8	7	34	Steel	66	26	27	26	Steel
35	7	6	35	Steel	67	27	28	27	Steel
36	6	5	36	Steel	68	28	29	28	Steel
37	5	4	37	Steel	69	29	30	29	Steel
38	4	3	38	Steel	70	30	31	30	Steel
39	3	2	39	Steel	71	31	32	31	Steel
40	2	1	40	Steel	72	32	33	32	Steel
41	21	22	1	Conc.	73	33	34	33	Steel
42	22	23	2	Conc.	74	34	35	34	Steel
43	23	24	3	Conc.	75	35	36	35	Steel
44	24	25	4	Conc.	76	36	37	36	Steel
45	25	26	5	Conc.	77	37	38	37	Steel
46	26	27	6	Conc.	78	38	39	38	Steel
47	27	28	7	Conc.	79	39	40	39	Steel
48	28	29	8	Conc.	80	40	41	40	Steel

Table B-3   Section properties.

Section No.	Material type	Area (in²)	Moment of inertia (in⁴)	Section No.	Material type	Area (in²)	Moment of inertia (in⁴)
1	Conc.	735	15,720	21	Steel	5.84	110
2	Conc.	740	16,063	22	Steel	5.84	113
3	Conc.	751	16,765	23	Steel	5.84	119
4	Conc.	767	17,854	24	Steel	5.84	128
5	Conc.	788	19,378	25	Steel	5.84	141
6	Conc.	815	21,401	26	Steel	5.84	157
7	Conc.	847	24,005	27	Steel	5.84	179
8	Conc.	885	27,298	28	Steel	5.84	206
9	Conc.	927	31,409	29	Steel	5.84	239
10	Conc.	975	36,499	30	Steel	5.84	279
11	Conc.	1,028	42,757	31	Steel	5.84	327
12	Conc.	1,087	50,411	32	Steel	5.84	384
13	Conc.	1,150	59,729	33	Steel	5.84	451
14	Conc.	1,219	71,022	34	Steel	5.84	530
15	Conc.	1,293	84,653	35	Steel	5.84	623
16	Conc.	1,371	101,040	36	Steel	5.84	729
17	Conc.	1,455	120,660	37	Steel	5.84	852
18	Conc.	1,544	144,050	38	Steel	5.84	993
19	Conc.	1,638	171,830	39	Steel	5.84	1,153
20	Conc.	1,736	204,700	40	Steel	5.84	1,334

Table B-4   Dead loads.

Node No.	Arch (kips)	Fill (kips)	Total (kips)	Node No.	Arch (kips)	Fill (kips)	Total (kips)
1	1.46	1.09	2.55	12	2.08	2.88	4.96
2	1.47	1.10	2.57	13	2.20	3.21	5.41
3	1.48	1.15	2.63	14	2.32	3.55	5.88
4	1.51	1.23	2.74	15	2.46	3.92	6.38
5	1.55	1.33	2.88	16	2.61	4.31	6.91
6	1.59	1.47	3.06	17	2.76	4.71	7.47
7	1.65	1.64	3.29	18	2.93	5.13	8.06
8	1.71	1.83	3.55	19	3.10	5.56	8.66
9	1.79	2.06	3.85	20	3.29	6.01	9.29
10	1.88	2.31	4.18	21	1.69	3.12	4.81
11	1.97	2.58	4.56				

Note: Dead loads are symmetric about crown.

Table B-5   Live loads.

Node No.	Live load (kips)	Node No.	Live load (kips)
1	1.42	12	1.37
2	1.42	13	1.36
3	1.41	14	1.36
4	1.41	15	1.35
5	1.41	16	1.34
6	1.41	17	1.32
7	1.40	18	1.31
8	1.40	19	1.30
9	1.39	20	1.29
10	1.39	21	0.64
11	1.38		

APPENDIX C: Campbell's Bridge Structural Model Definition

Table C-1   Nodal coordinates.

Node No.	X coordinate (ft)	Y coordinate (ft)	Node No.	X coordinate (ft)	Y coordinate (ft)
1	36	-8.757	9	-36	-8.757
2	30	-5.965	10	40	-3.925
3	20	-2.595	11	30	-2.699
4	10	-0.641	12	20	-1.474
5	0	0	13	-20	-1.474
6	-10	-0.641	14	-30	-2.699
7	-20	-2.595	15	-40	-3.925
8	-30	-5.965			

Table C-2   Member definitions.

Member No.	Joint 1	Joint 2	Section No.	Section type	Member No.	Joint 1	Joint 2	Section No.	Section type
1	1	2	1	A1	10	11	12	6	D2
2	2	3	2	A2	11	12	4	7	D3
3	3	4	3	A3	12	6	13	7	D3
4	4	5	4	A4	13	13	14	6	D2
5	5	6	4	A4	14	14	15	5	D1
6	6	7	3	A3	15	2	11	8	V1
7	7	8	2	A2	16	3	12	9	V2
8	8	9	1	A1	17	7	13	9	V2
9	10	11	5	D1	18	8	14	8	V1

Table C-3   Section properties.

Section No.	Section type	Area (in²)	Moment of inertia (in⁴)
1	A1	1,303	131,500
2	A2	1,155	89,800
3	A3	1,031	62,300
4	A4	2,343	558,000
5	D1	2,350	104,200
6	D2	2,350	104,200
7	D3	2,350	104,200
8	V1	1,493	102,300
9	V2	1,493	102,300

Table C-4   Dead loads.

Member No.	Dead load (kip/ft)	Joint No.	Dead load (kips)
1	-1.26	2	-9.05
2	-1.11	3	-4.53
3	-0.98	4	-3.89
4	-3.68	5	-2.88
5	-3.68	6	-3.89
6	-0.98	7	-4.53
7	-1.11	8	-9.05
8	-1.26		
9	-2.8		
10	-2.8		
11	-2.8		
12	-2.8		
13	-2.8		
14	-2.8		